103
11-3

UC-33 Drawer No. 1638

AEC Report No.
TE4125-1

Thermo Electron
Report No. TE4122-12-71

TOPICAL REPORT

THERMIONIC PERFORMANCE OF FLUORIDE CVD TUNGSTEN-NIOBIUM CONVERTER

F. Rufeh and D. Lieb

THIS DOCUMENT CONFIRMED AS
UNCLASSIFIED
DIVISION OF CLASSIFICATION
BY J H Kahn Jamb
DATE 11/17/70

June 1970

Thermo Electron Corporation
85 First Avenue
Waltham, Massachusetts 02154

prepared for

U. S. Atomic Energy Commission

Space Nuclear Systems Division
Contract AT(30-1)-4125

Lester K. Price, AEC Project Manager

DISTRIBUTION OF THIS DOCUMENT IS UNLIMITED

P7441

DISCLAIMER

This report was prepared as an account of work sponsored by an agency of the United States Government. Neither the United States Government nor any agency Thereof, nor any of their employees, makes any warranty, express or implied, or assumes any legal liability or responsibility for the accuracy, completeness, or usefulness of any information, apparatus, product, or process disclosed, or represents that its use would not infringe privately owned rights. Reference herein to any specific commercial product, process, or service by trade name, trademark, manufacturer, or otherwise does not necessarily constitute or imply its endorsement, recommendation, or favoring by the United States Government or any agency thereof. The views and opinions of authors expressed herein do not necessarily state or reflect those of the United States Government or any agency thereof.

DISCLAIMER

Portions of this document may be illegible in electronic image products. Images are produced from the best available original document.

LEGAL NOTICE

This report was prepared as an account of Government sponsored work Neither the United States, nor the Commission, nor any person acting on behalf of the Commission:

A. Makes any warranty or representation, expressed or implied, with respect to the accuracy, completeness, or usefulness of the information contained in this report, or that the use of any information, apparatus, method, or process disclosed in this report may not infringe privately owned rights; or

B. Assumes any liabilities with respect to the use of, or for damages resulting from, the use of any information, apparatus, method, or process disclosed in this report.

As used in the above, "person acting on behalf of the Commission" includes any employee or contractor of the Commission, or employee of such contractor, to the extent that such employee or contractor of the Commission, or employee of such contractor, prepares, disseminates, or provides access to, any information pursuant to his employment or contract with the Commission, or his employment with such contractor.

AVAILABILITY NOTICE

Printed in USA. Price $3.00. Available from the Clearinghouse for Federal Scientific and Technical Information, National Bureau of Standards, U. S. Department of Commerce, Springfield, Virginia, 22151.

AEC Report No.
TE4125-1

Thermo Electron
Report No. TE4122-12-71

TOPICAL REPORT

THERMIONIC PERFORMANCE OF FLUORIDE CVD TUNGSTEN-NIOBIUM CONVERTER

F. Rufeh and D. Lieb

June 1970

Thermo Electron Corporation
85 First Avenue
Waltham, Massachusetts 02154

prepared for

U S. Atomic Energy Commission

Space Nuclear Systems Division
Contract AT(30-1)-4125

Lester K. Price, AEC Project Manager

LEGAL NOTICE

This report was prepared as an account of work sponsored by the United States Government. Neither the United States nor the United States Atomic Energy Commission, nor any of their employees, nor any of their contractors, subcontractors, or their employees, makes any warranty, express or implied, or assumes any legal liability or responsibility for the accuracy, completeness or usefulness of any information, apparatus, product or process disclosed, or represents that its use would not infringe privately owned rights.

ACKNOWLEDGMENTS

The authors acknowledge the contributions of Norman Adrian in design, and Frank Campagna and Emil Ameen in the construction of the converter.

TABLE OF CONTENTS

Section		Page
I	INTRODUCTION	1
II	CONVERTER CONSTRUCTION	2
III	VACUUM WORK FUNCTION	4
IV	PERFORMANCE MEASUREMENT	5
V	TRANSIENT BEHAVIOR	7
VI	REFERENCES	11

Appendix

A	TEST CONVERTER	A-1
B	FAMILIES OF VOLT-AMPERE CHARACTERISTICS	B-1

I. INTRODUCTION

Fluoride vapor-deposited tungsten has been shown to form a mechanically stable and easily fabricated thermionic emitter structure. It has been used with a niobium collector in many fixed-spacing hardware converters for both in-pile and out-of-pile life tests. A complete performance map of this electrode pair showing the dependence of output power on converter parameters has not been available. Such data are useful for diagnosis and evaluation of the life test results. In this work, parametric data are obtained in a research, variable-spacing thermionic converter for a wide range of converter parameters.

Attempts were also made to measure the cesiated work function of the electrodes. The transient effects observed showed that, unlike other materials, the emission characteristics of this emitter depend on its temperature history preceding the test. This dependence was attributed to the diffusion of an impurity element, possibly carbon, in the fluoride tungsten material to the emitter surface. It is known that the performance of fluoride tungsten emitters is considerably lower than that of other emitters (e. g., chloride tungsten). The present data indicate that the performance at low temperatures (less than 1800°K) would have been even lower if additives were not diffusing through the emitter. The data presented here are believed to be representative of fluoride tungsten emitters.

II CONVERTER CONSTRUCTION

The emitter was fluoride vapor-deposited by San Fernando Laboratories, electrical discharge machined to rough dimensions and then surface ground It was then vacuum-fired for one hour at 1980°C A photomicrograph of the resulting surface is shown in Figure 1. X-ray diffraction measurements of the annealed emitter showed a high degree of <100> orientation with a relatively large grain size. Figure 2 summarizes the degree of surface orientation about the <100> planes

A schematic of the converter is shown in Figure 3 The collector and guard body were machined from molybdenum bar stock. The active area was formed by brazing a slice from niobium bar stock to the molybdenum body. The entire assembly was then machined to the final dimensions A niobium emitter shield is used as both a radiation and plasma shield and a getter.

The electrode surface areas are 2 cm^2 for the collector and 3 cm^2 for the emitter. The guard ring extends approximately 60 mils beyond the edges of the projected emitter area Spacing is adjusted and measured by three micrometer screws (shown in Figure 2) fastened to the emitter and guard support structures. Spacing can be read to a precision of about 0. 5 mil, with a minimum value of 0. 25 to 0. 5 mils. A more detailed description is given in Appendix A and in Reference 1.

Emitter temperature is determined by optical pyrometry on a hohlraum in the back surface of the emitter; temperature readings are corrected to surface values using the bombardment power input to give the heat flux. The accuracy of the measurements is ± 10°K.

Thermocouples close to the respective surfaces are provided for collector and guard temperature measurement. Reference 2 describes the temperature measurement and the required corrections.

The collector and guard structures were vacuum-fired before final assembly. Particular care was taken throughout outgassing to maintain the pump pressure below 5×10^{-7} torr. If the pressure exceeds this value considerably during some stage of the outgassing, oxides might be formed on the internal surfaces and release oxygen during the subsequent thermionic operation of the converter.

To avoid introducing impurities with cesium, a metal capsule containing predistilled cesium was used; this capsule was prepared by refluxing the cesium while pumping through a cold trap.[1] With this system the converter was not exposed to any additional contaminants during cesiation

III. VACUUM WORK FUNCTION

The vacuum work function of a similarly prepared emitter was 4.66 eV. The value obtained in the converter for this emitter was 4.7 eV. These values are higher than expected for fluoride tungsten (~4.6). In view of the extreme sensitivity of low work function tungsten to oxygen contamination, and because the background pressures were higher than usual during the measurements, these values are believed to be erroneous.

IV. PERFORMANCE MEASUREMENT

Before performance tests were initiated, the cesiated converter was examined for oxygen contamination (as described in Reference 1). Figure 4 shows the collector family obtained from this test. The curves only shift parallel to the voltage axis, indicating that a change in saturation current due to oxygen released from the collectors did not occur.

Families of volt-ampere characteristics were obtained by changing the cesium pressure while the other converter parameters were held constant. The data cover the emitter temperature range of 1600 to 2000 °K and the interelectrode spacing range of 0.5 to 40 mils. Typical cesium families for the interelectrode spacing of 10 mils are shown in Figures 5 through 9 and the data for other interelectrode spacings are shown in Appendix B. The emitter temperature indicated represents the temperature at the emitting surface, and the collector temperatures were chosen to be in the vicinity of the optimum values. The output voltage is measured from a voltage tap at the cold end of the emitter sleeve and requires a correction of 1.5 mV per amp/cm^2 for conversion to electrode voltage. In order to facilitate the use of these data for analyses and correlations of converter parameters, the cesium pressure (P) and the interelectrode spacings (d) in these data are chosen to provide Pd products of . . . , 5, 10, 20, 40, . . . mil-torr. A table for conversion from cesium reservoir temperature to cesium pressure is shown in Table I, and the envelopes of the cesium families are summarized in Figures 10 through 14. Each curve in these figures

represents the optimized performance with respect to cesium pressure and collector temperature. The fully optimized performance is shown in Figure 15.

The performance of the present emitter material is compared with that of "single-crystal" ⟨110⟩ tungsten and duplex tungsten in Figure 16 This comparison shows that fluoride tungsten is a poor emitter. In Figures 17, 18 and 19, the low performance is further emphasized. The small values of optimum spacing are additional evidence that the emitter requires a relatively high value of cesium pressure for a given operating current. The performance of this combination is also consistent with that observed in hardware devices and can be used for comparisons.

TABLE I

CESIUM VAPOR PRESSURE

Temperature		Pressure	Temperature		Pressure
°C	°K	Torr	°C	°K	Torr
163	436	0.016	266	539	0.71
171	444	0.022	278	551	1.0
179	452	0.031	291	564	1.4
187	460	0.044	304	577	2.0
196	469	0.063	318	591	2.8
204	477	0.088	332	605	4.0
214	487	0 13	347	620	5.7
223	496	0.178	363	636	8.0
234	507	0.25	380	653	11.
244	517	0.35	398	671	16.
255	528	0.50	416	689	23.

V TRANSIENT BEHAVIOR

During the cesiated work function measurements on this converter, certain inconsistencies were observed in the data Analysis of the converter behavior showed that the irreproducibility of the work function measurements was caused by the dependence of electron emission on the temperature history of the emitter. When the emitter was flashed at 2000°K for 10 minutes and then suddenly reduced to 1700°K, the saturated emission current greatly increased with time Figures 22 and 23 show the time dependence of current and the corresponding work function depression at the cesium temperature of 480°K. Data obtained at higher cesium temperatures showed the same qualitative features but the work function depression was considerably less.

The time constant involved is much larger than that for the desorption of cesium; therefore, another element or "additive" must be involved. Further examination of the converter did not show dependence of the emission on the temperature of the converter components such as the collector, the guard or the emitter ring, indicating that the "additive" is probably diffusing from the emitter body to the emitter surface.

Chemical analysis of the fluoride tungsten material from which the emitter was made was performed by Dr. L. Yang of Gulf General Atomic. The results are:

fluorine	3	ppm/weight
carbon	22	ppm/weight
hydrogen	0.6	ppm/weight
oxygen	2.2	ppm/weight
nitrogen	0.8	ppm/weight

These quantities are not unusual for CVD fluoride tungsten. The observed emission characteristics can be caused by fluorine, oxygen or possibly by carbon. This behavior is qualitatively similar to the emission characteristics of thoriated tungsten emitters. There are two competing processes that control the coverage of the additive on the surface: diffusion of the additive through the emitter material to the surface, and evaporation of the additive from the surface. According to Langmuir's[3] work, the rate of change of coverage with time is given by

$$N \frac{d\theta}{dt} = DG - \nu\theta , \tag{1}$$

where θ is the coverage, N is the number of additive atoms per cm^2 in a complete monatomic adsorbed film (θ-1), D is the diffusion coefficient of the additive in the metal, G is the concentration gradient just under the adsorbed film and $\nu\theta$ is the evaporation rate from the surface at θ.

Integration of the above equation with the boundary conditions

$$t = 0 ; \qquad \theta = \theta_0 \tag{2}$$

$$t = \infty ; \qquad \theta = \frac{DG}{\nu} = \theta_\infty \tag{3}$$

yields

$$\theta = \frac{DG}{\nu} + \left(\theta_0 - \frac{DG}{\nu}\right) \exp\left(-t/\tau\right) \tag{4}$$

where

$$\tau = \frac{N}{\nu} \tag{5}$$

Assuming a linear relationship between work function and coverage,

$$\theta = a\phi + b , \tag{6}$$

and using the Richardson Equation,

$$J = A T^2 \exp\left(-\phi/kT\right), \tag{7}$$

equation 4 becomes

$$\frac{\ln J_\infty - \ln J}{\ln J_\infty - \ln J_0} = \exp\left(-t/\tau\right), \tag{8}$$

where J_0 and J_∞ represent the current density at $t = \theta$ and $t = \infty$.

As the emitter temperature is increased from 1700°K to 2000°K, the evaporation rate increases more rapidly than the product DG; hence, θ_∞ decreases (see eq. 3). Subsequent quenching to 1700°K results in a low initial current J_0. Current density then slowly increases with time to the value of J_∞ (eq. 8). Rewriting equation 8 gives

$$\ln\left(\ln J_\infty - \ln J\right) = \ln\left(\ln J_\infty - \ln J_0\right) - \frac{t}{\tau} . \tag{9}$$

A plot of $\ln\left(\ln J_\infty - \ln J\right)$ as a function of time should yield a straight line with a slope given by $-1/\tau$. Such a plot is shown in Figure 24.

using the data in Figure 23, for the flashing temperature of 2000°K and an activation temperature of 1700°K. Similar results were observed at other activation temperatures. The calculated time constants are transformed into the evaporation rates of the additives from the metal surfaces and summarized in Figure 25. Also shown are the time constants for oxygen[4] and fluorine[5] on tungsten. Data are not available for the evaporation rate of carbon or tungsten. The available data on carbon[6] cannot be transformed into the evaporation rate, although reported time intervals similar to those in the present work have been observed. Furthermore, the present data show a discontinuity at the temperature of 1730°K. The discontinuity is not due to experimental errors, since the data are reproducible; rather, it appears to be due to a phase transformation. Baker and Gaines[6] detected two emission states corresponding to WC and W_2C.

The power data reported in the previous section correspond to the performance after equilibrium conditions are reached for each emitter temperature. An experiment was carried out to determine the effect of the additive on the power output of the converter. The emitter temperature was flashed at 2000°K for 10 minutes and then reduced to 1700°K, and a cesium family was obtained. Figure 26 shows the optimized cesium envelopes for these two families at the collector temperature of 670°K. The performance significantly improves with time after flashing. Although the cesium families were not obtained at optimum collector temperature, it appears that the performance of this converter at low temperatures would have been even worse if additives were not diffusing through the emitter. The power data reported in the previous section correspond to the performance after equilibrium conditions are reached for each emitter temperature.

VI. REFERENCES

1. D. Lieb, A. Donaker, and F. Rufeh, "Performance of a Thermionic Converter with a Nominal Single-Crystal ⟨110⟩ Tungsten Emitter and a Niobium Collector," Proceedings of the IEEE Thermionic Conversion Specialists Conference, Carmel, California, 1969.

2. D. Lieb, "Topical Report: Thermal Flux in a Research Parametric Converter," Thermo Electron Corporation Report No. TE4086-32-70, June 30, 1969.

3. I. Langmuir, Journal of Franklin Institute, Vol. CCXVII, No. 5, May, 1934.

4. I. Langmuir and D. Villars, J. Am. Chem. Society, Vol. LIII, No. 53, 486 (1931).

5. D. Lieb and S. Kitrilakis, Proceedings of the IEEE Thermionic Conversion Specialists Conference, Houston, Texas, 1966.

6. J. B. Baker and C. B. Gaines, Proceedings of the IEEE Thermionic Conversion Specialist Conference, Gatlinburg, Tennessee, 1963.

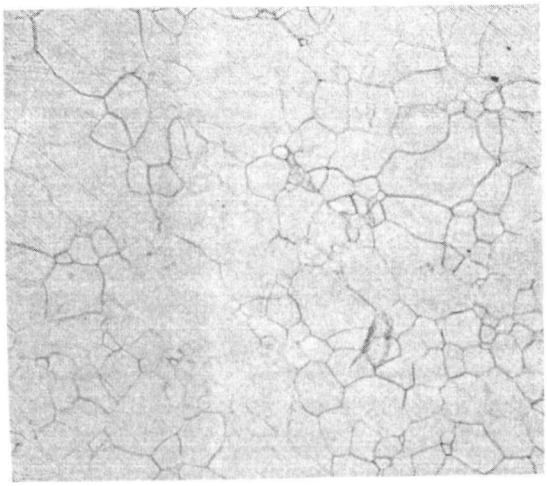

Figure 1. Photomicrograph of Representative Area of the Emitter.

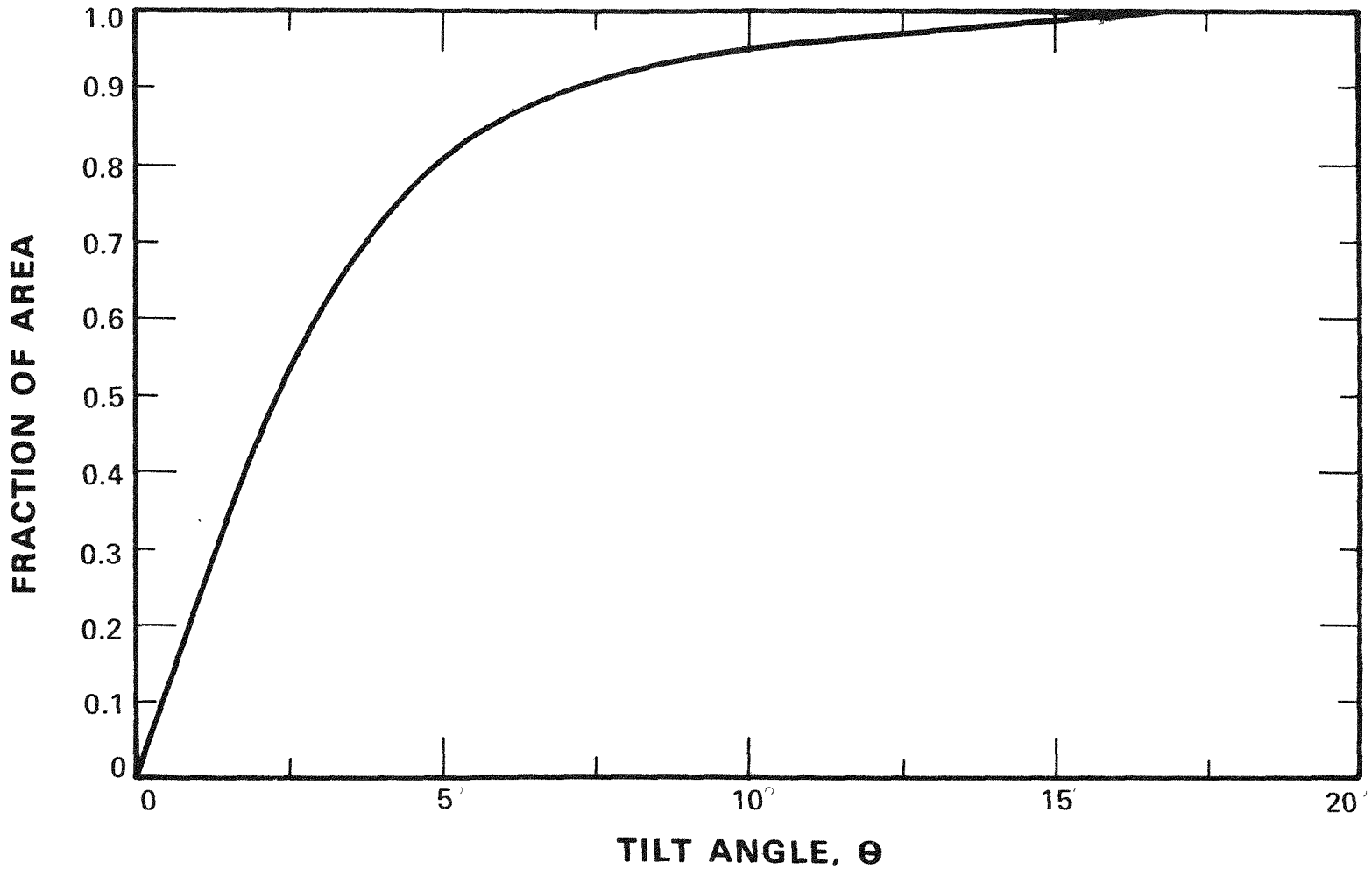

Figure 2. Pole Figure Showing the Fraction of Sample Area Having (100) Axes Lying Within Angle θ from Normal to Sample Surface.

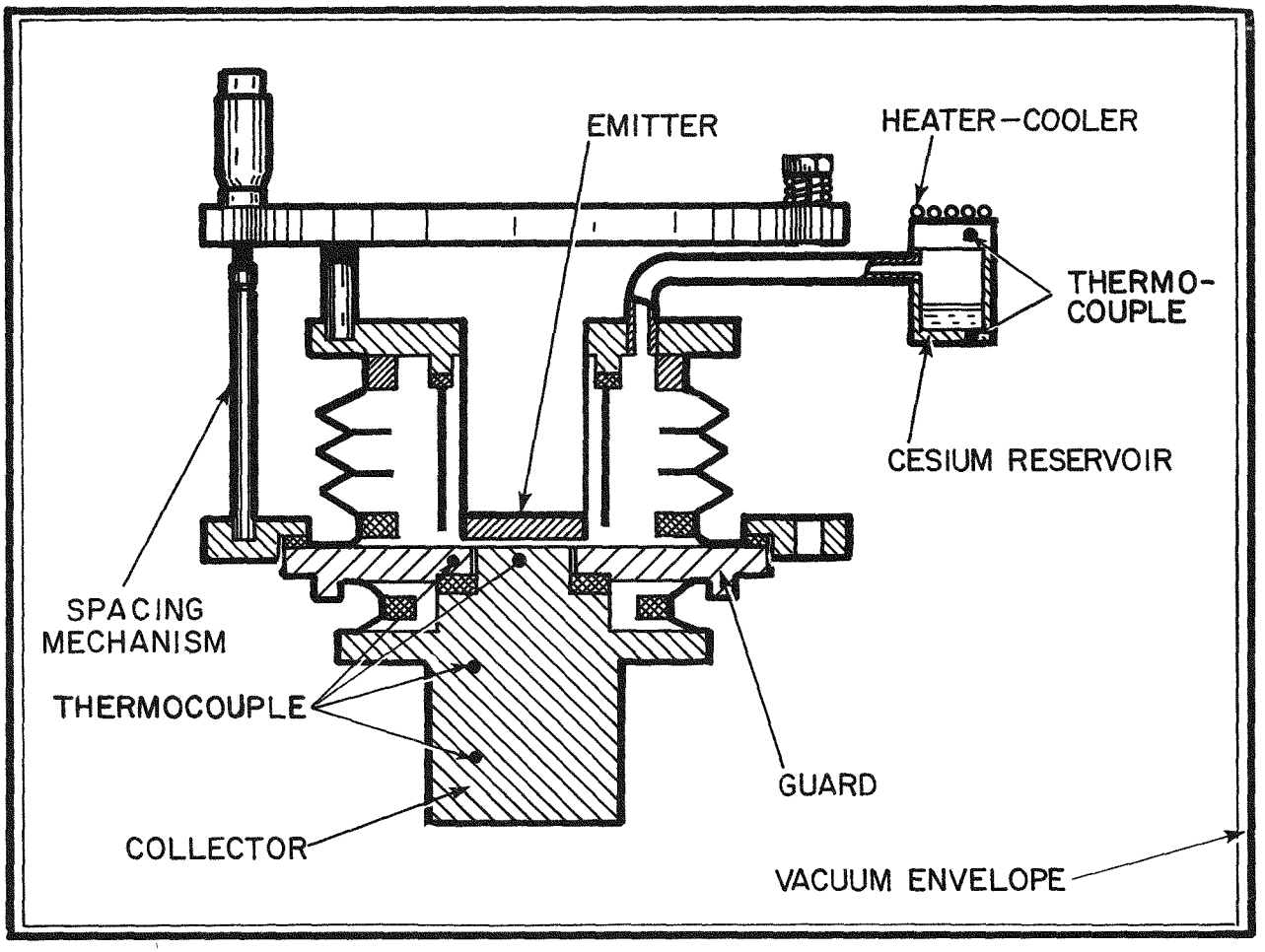

Figure 3. Schematic Diagram of a Research Thermionic Converter.

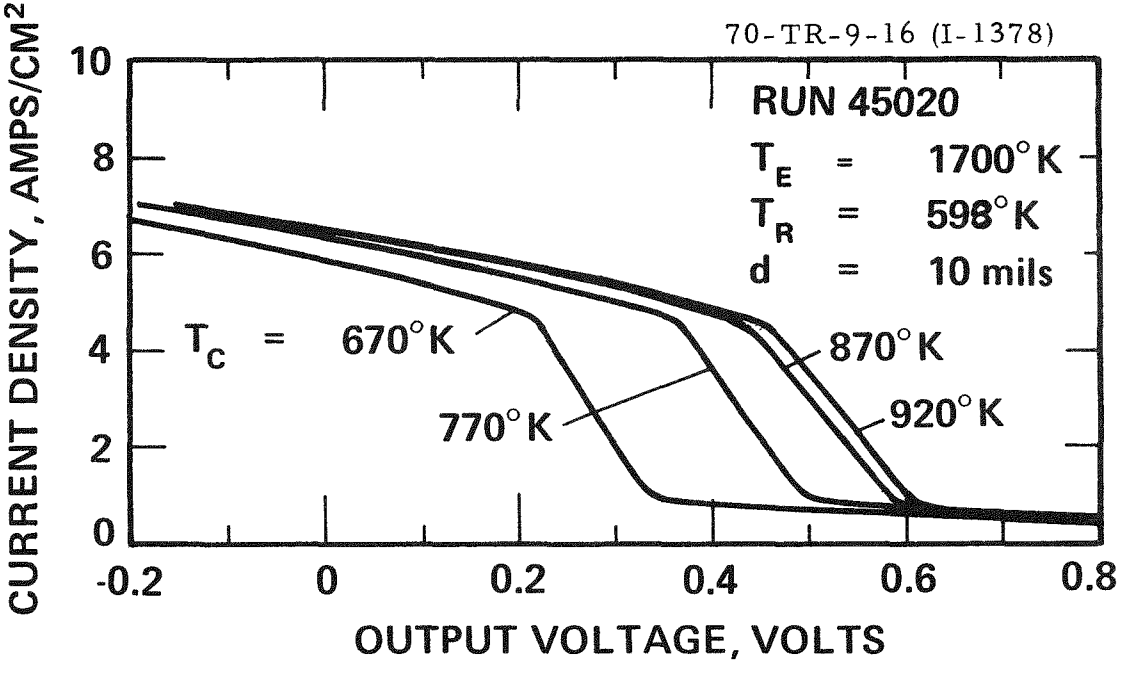

Figure 4. Typical Collector Family of I-V Characteristics.

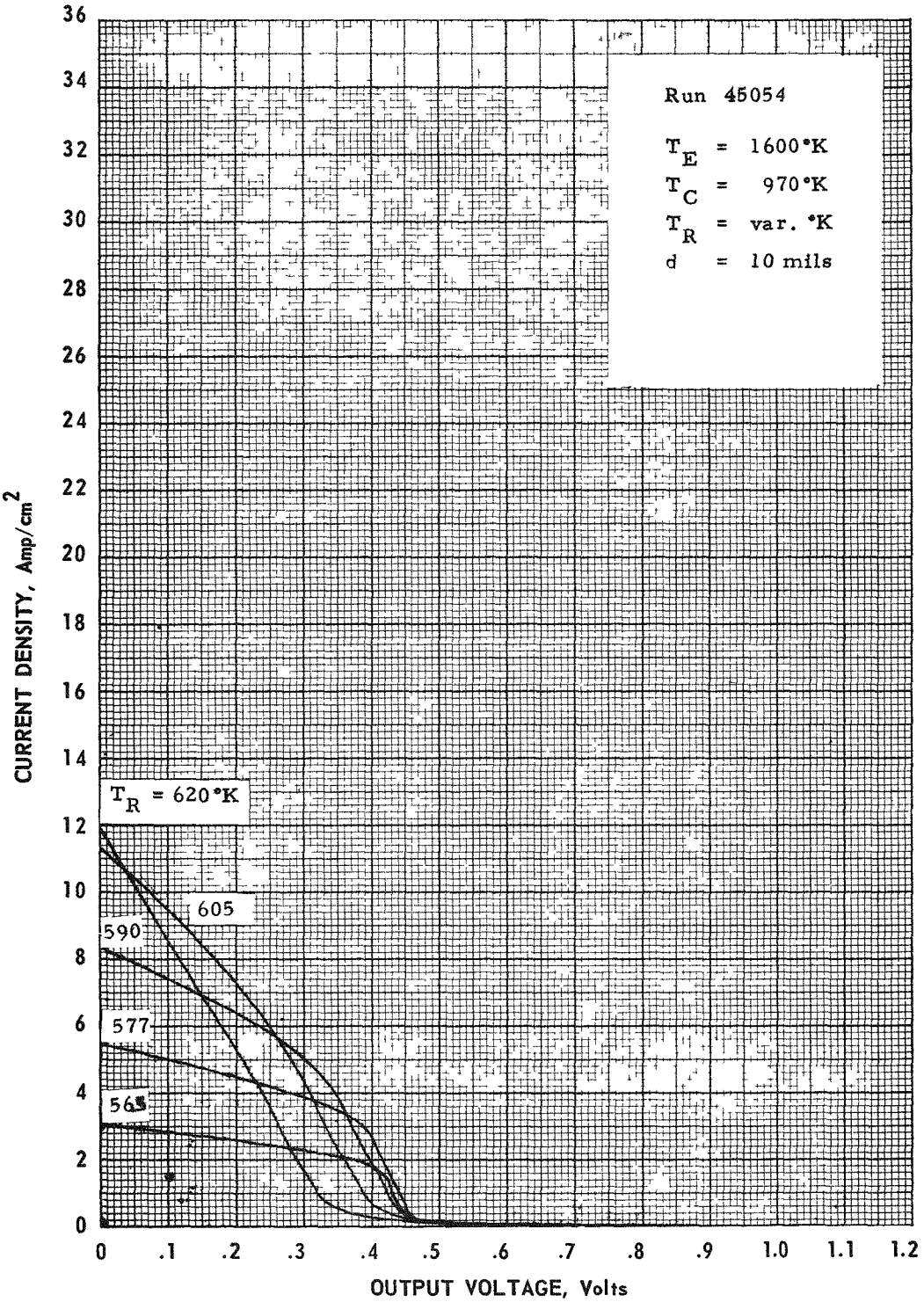

Figure 5. Variable Cesium Temperature Family at T_E = 1600°K.

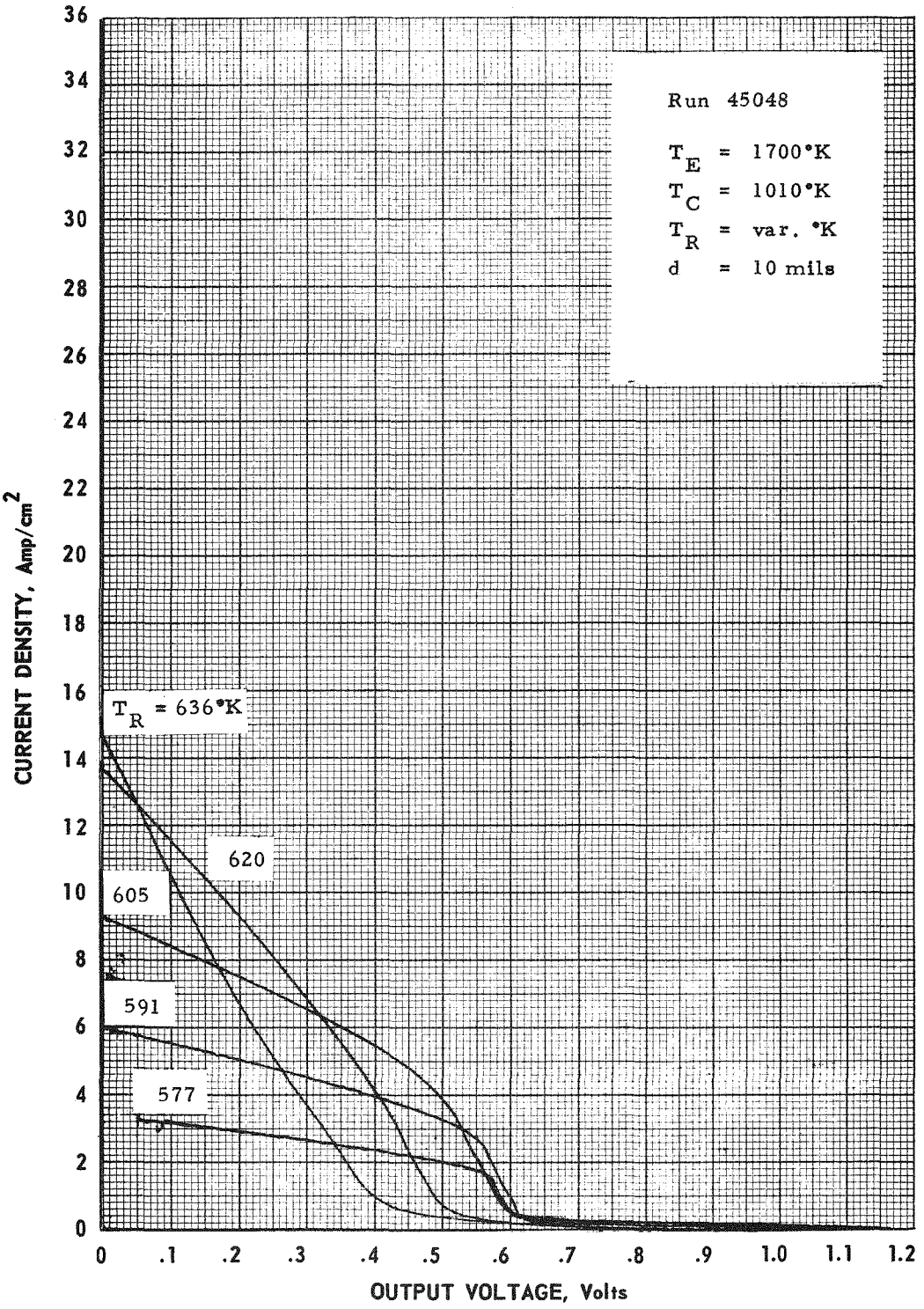

Figure 6. Variable Cesium Temperature Family at T_E = 1700°K.

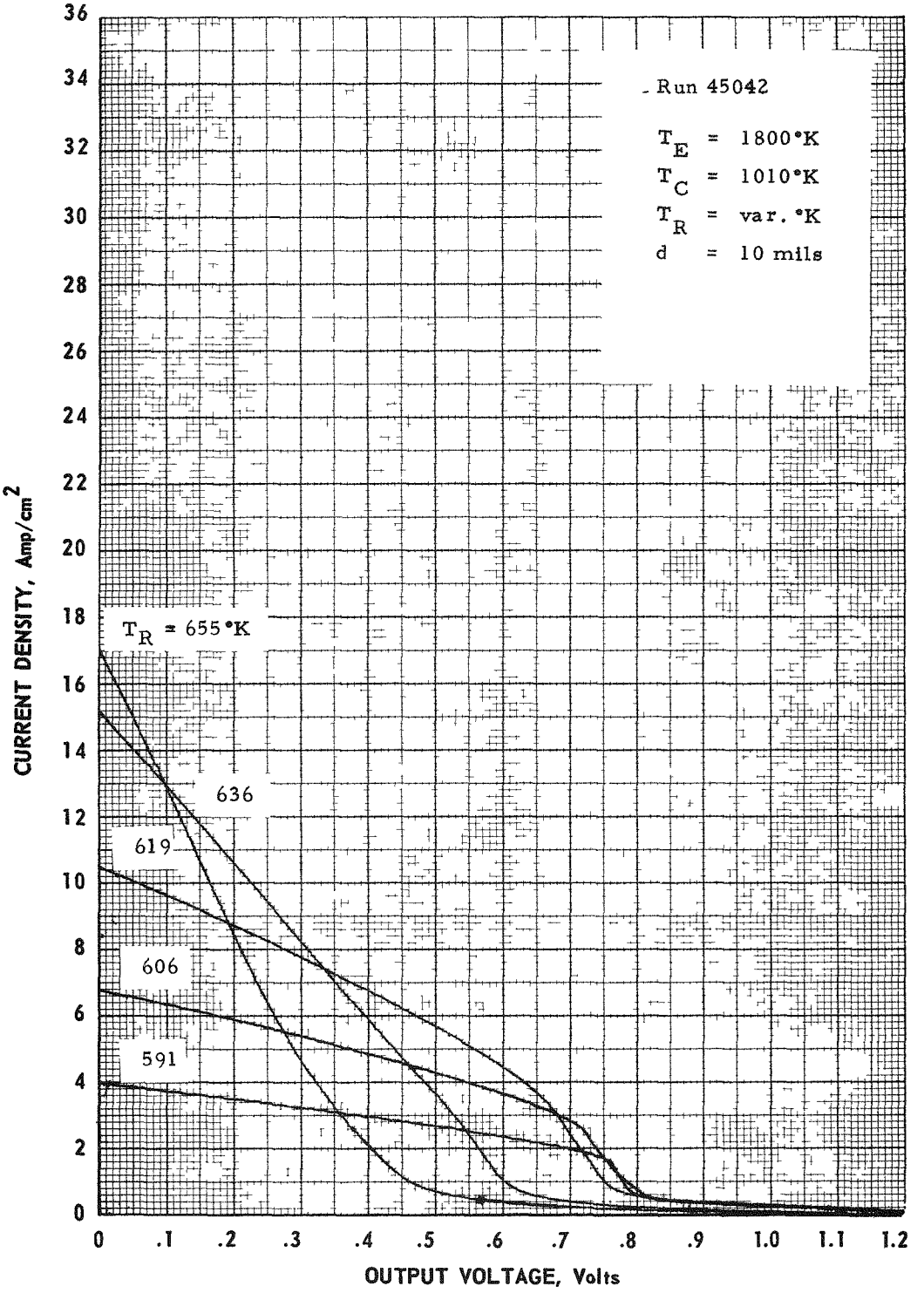

Figure 7. Variable Cesium Temperature Family at T_E = 1800°K.

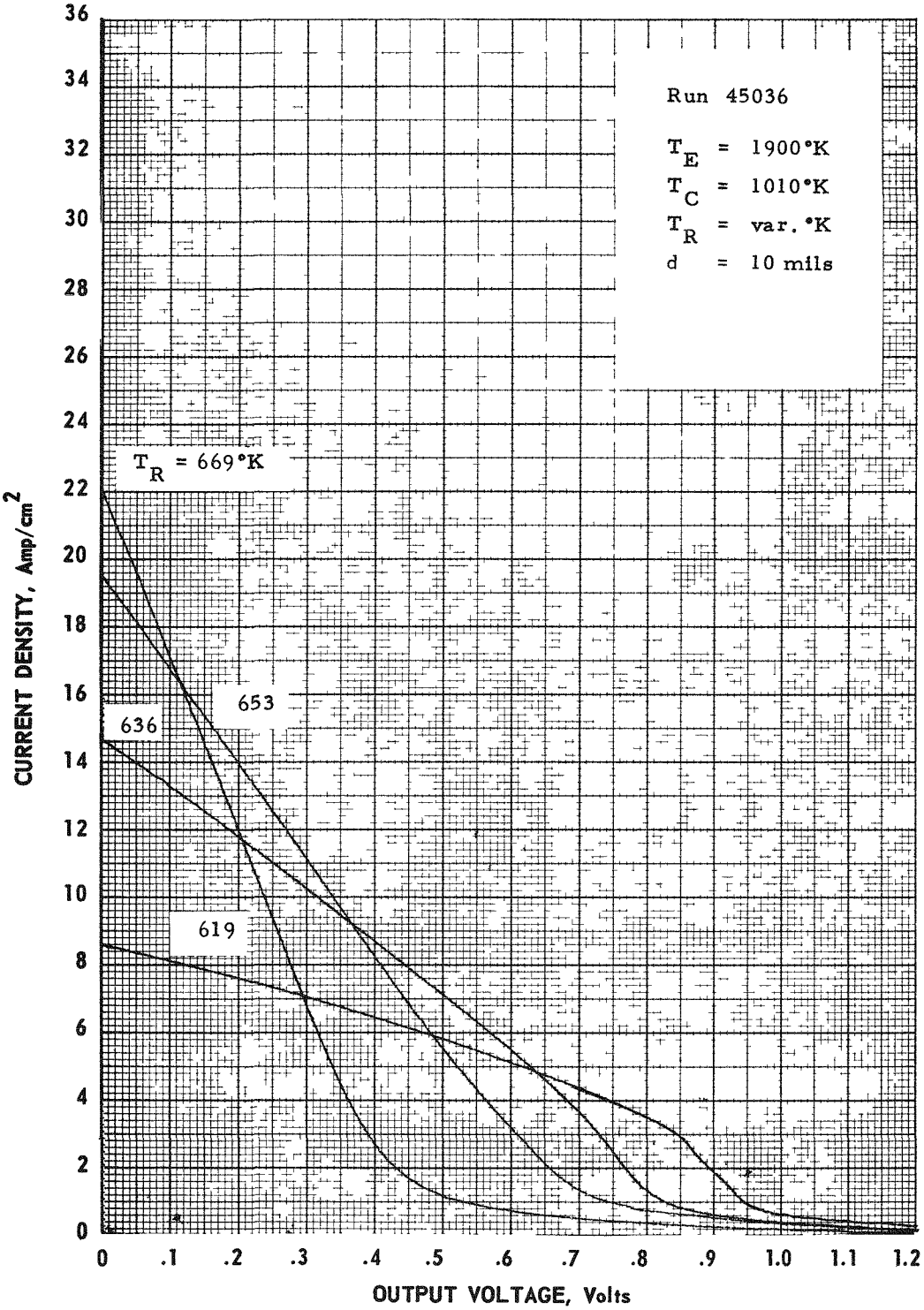

Figure 8. Variable Cesium Temperature Family at T_E = 1900°K.

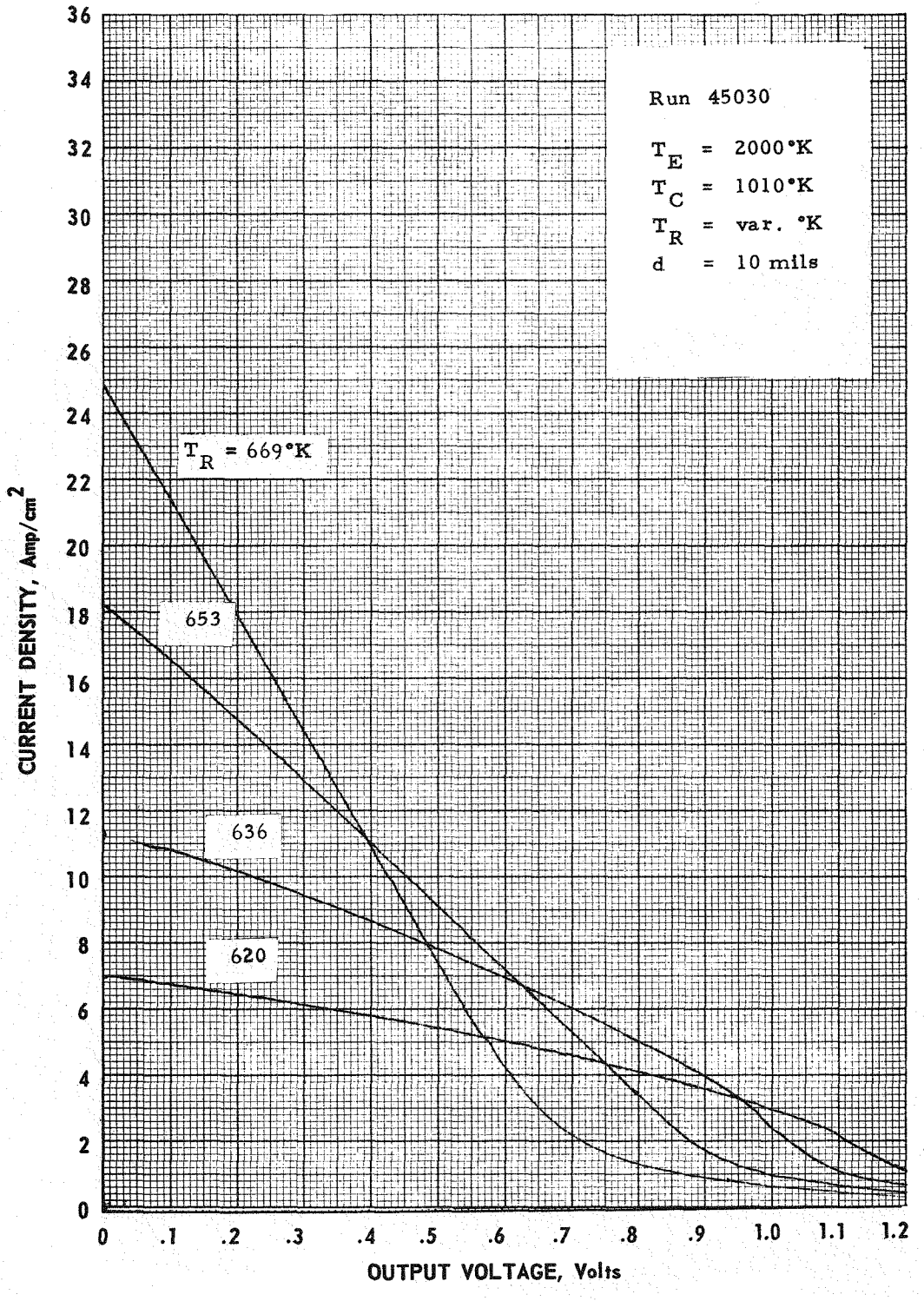

Figure 9. Variable Cesium Temperature Family at T_E = 2000°K.

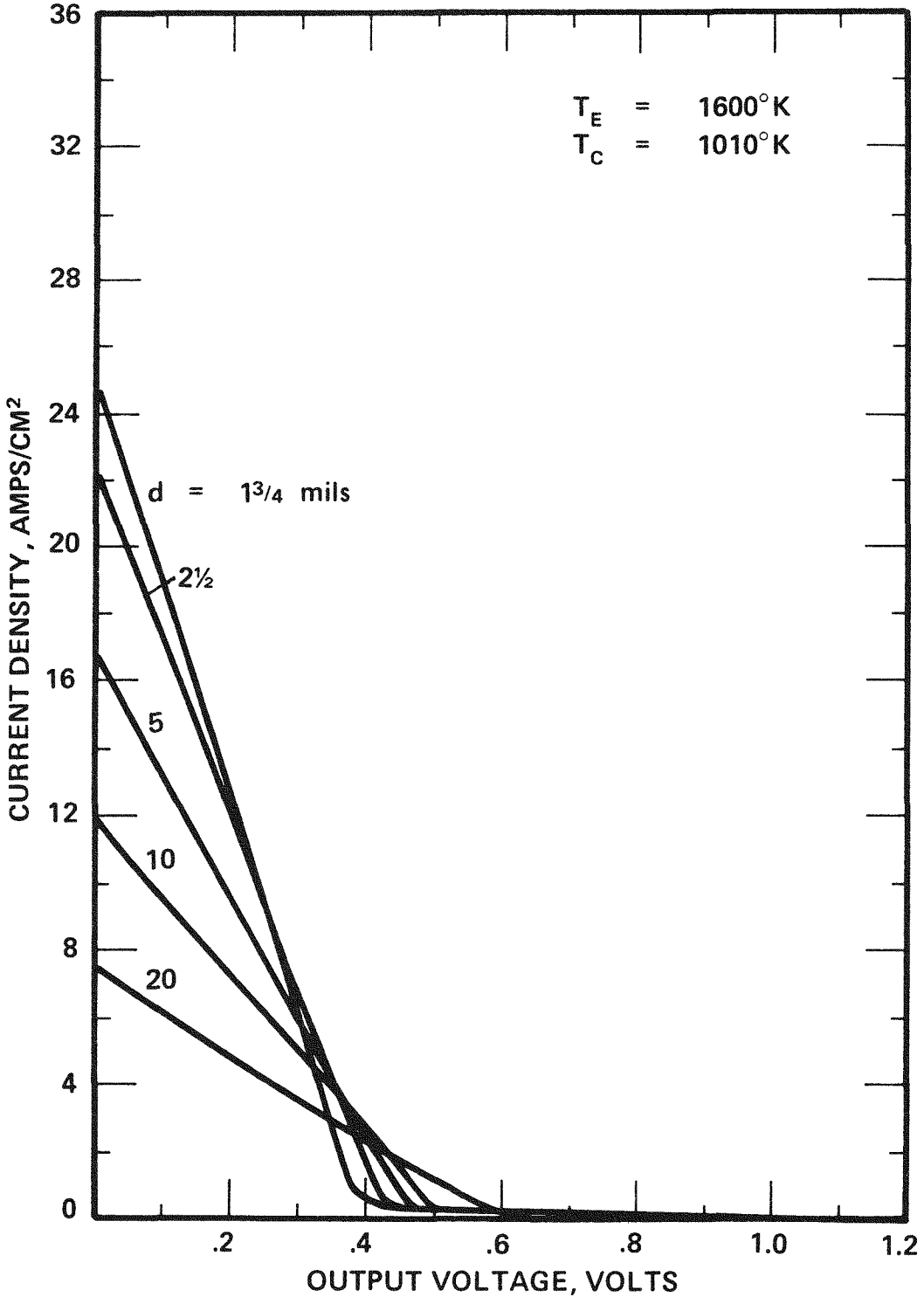

Figure 10. Cesium Optimized Performance for Several Interelectrode Spacings at T_E = 1600°K.

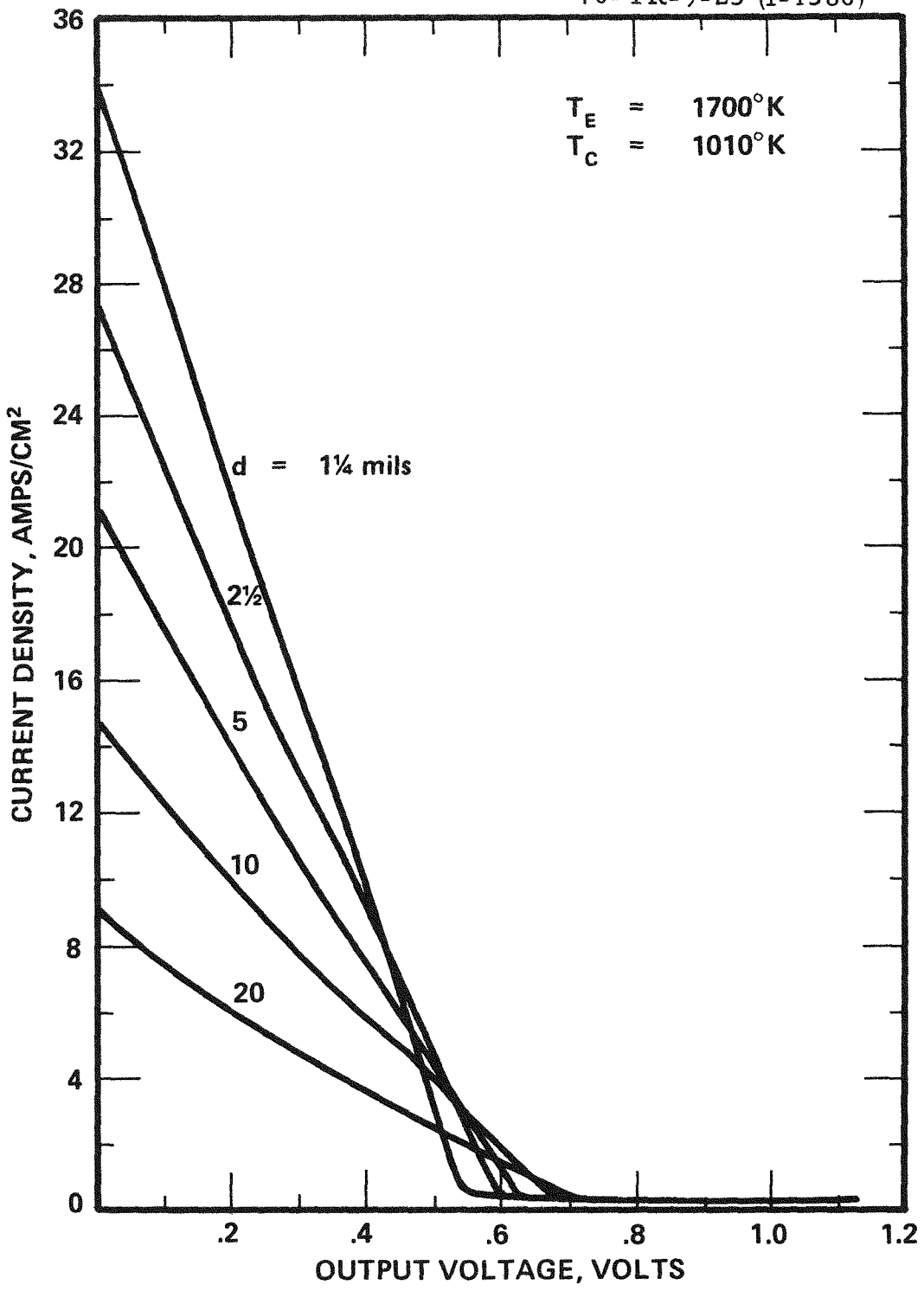

Figure 11. Cesium Optimized Performance for Several Interelectrode Spacings at T_E = 1700°K.

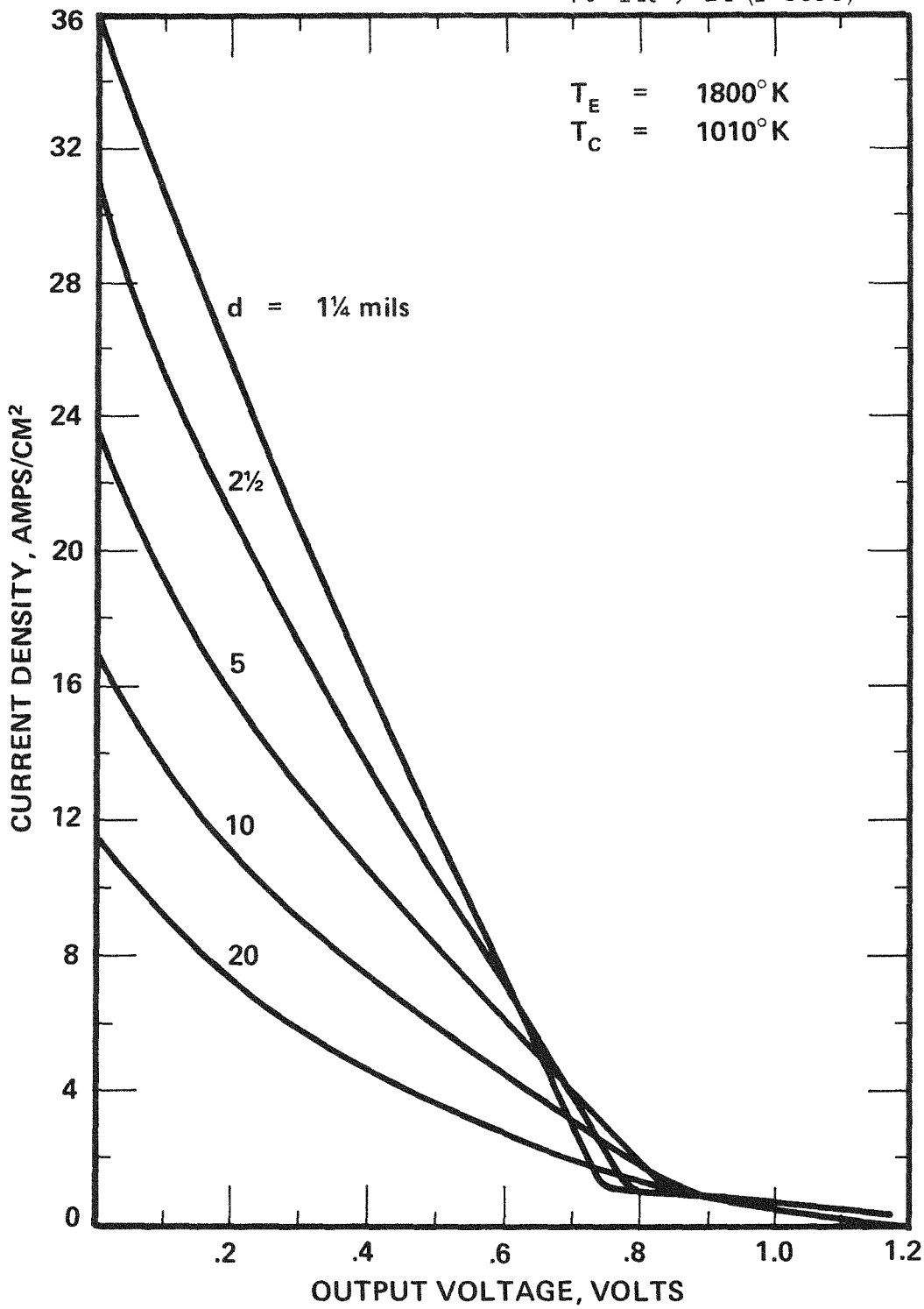

Figure 12. Cesium Optimized Performance for Several Interelectrode Spacings at T_E = 1800°K.

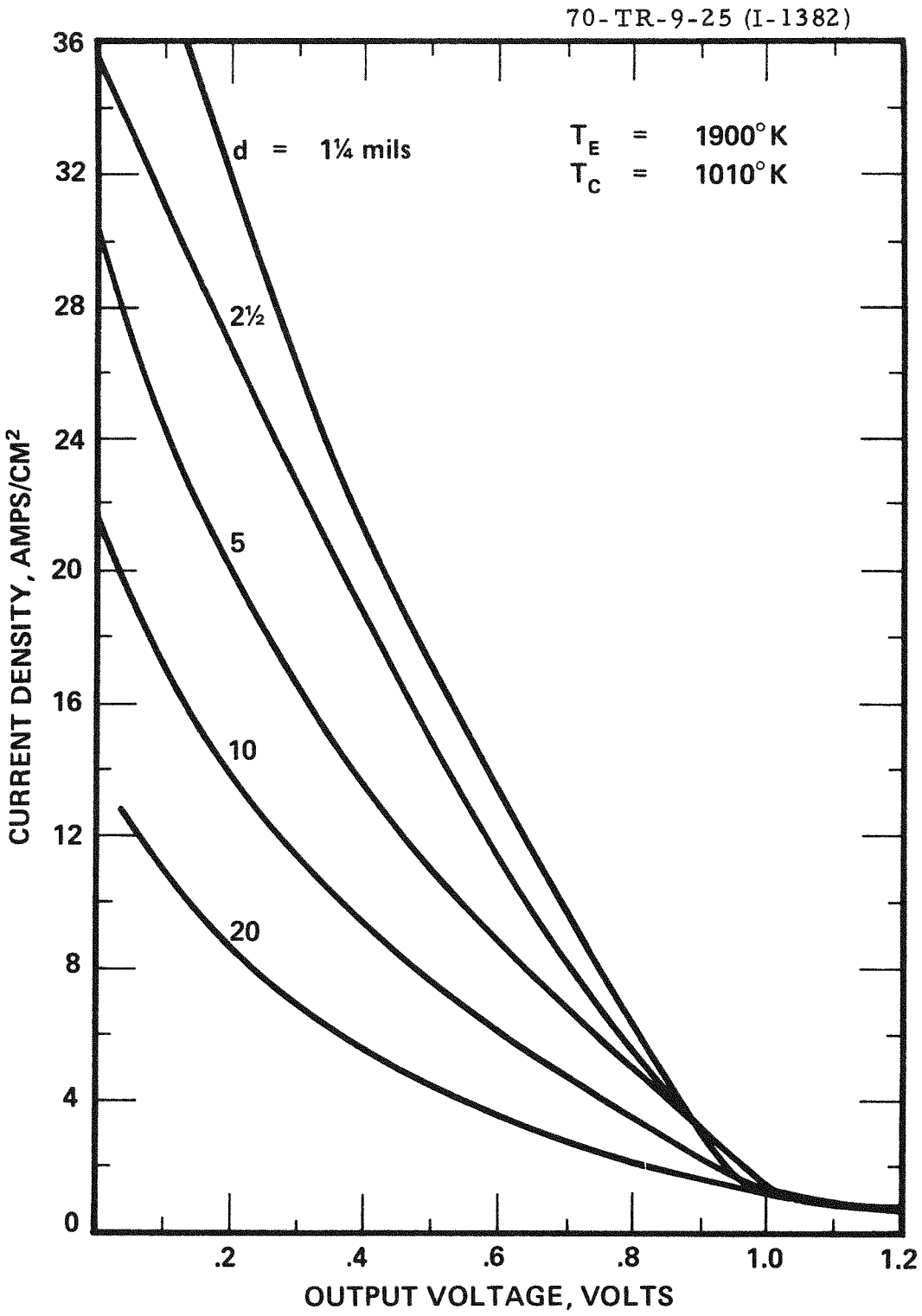

Figure 13. Cesium Optimized Performance for Several Interelectrode Spacings at T_E = 1900°K.

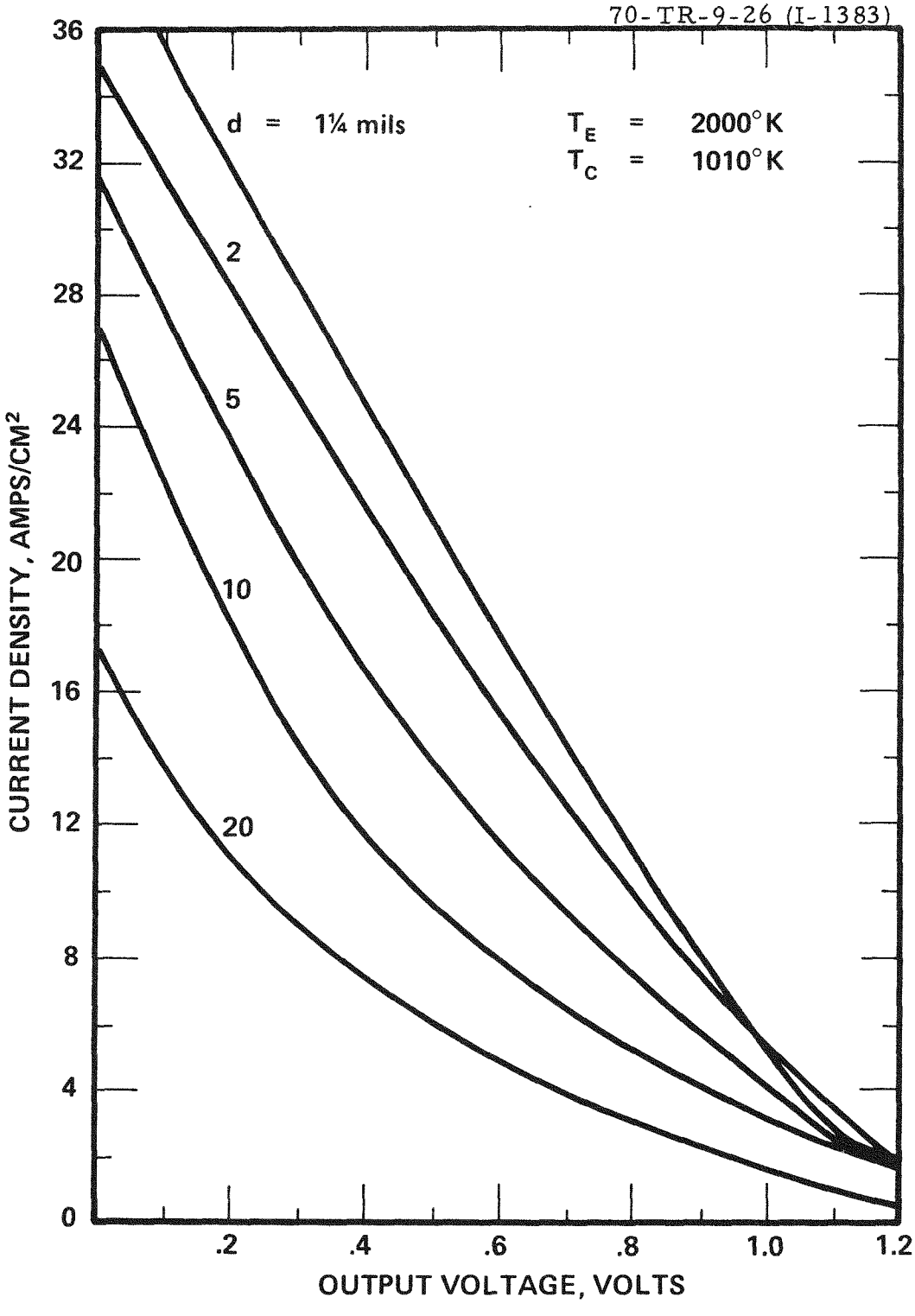

Figure 14. Cesium Optimized Performance for Several Interelectrode Spacings at T_E = 2000°K.

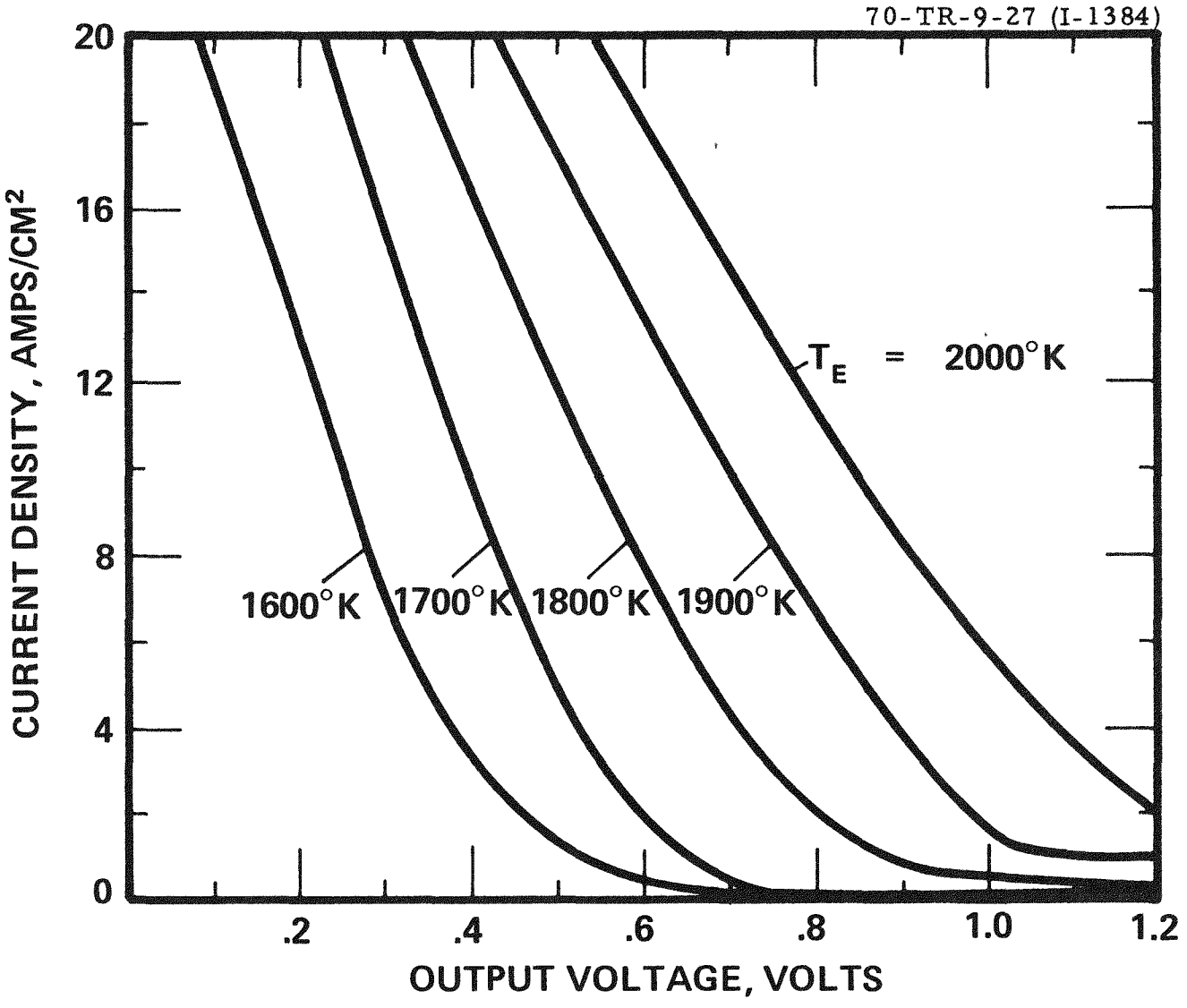

Figure 15. Fully Optimized Performance of Several Emitter Temperatures.

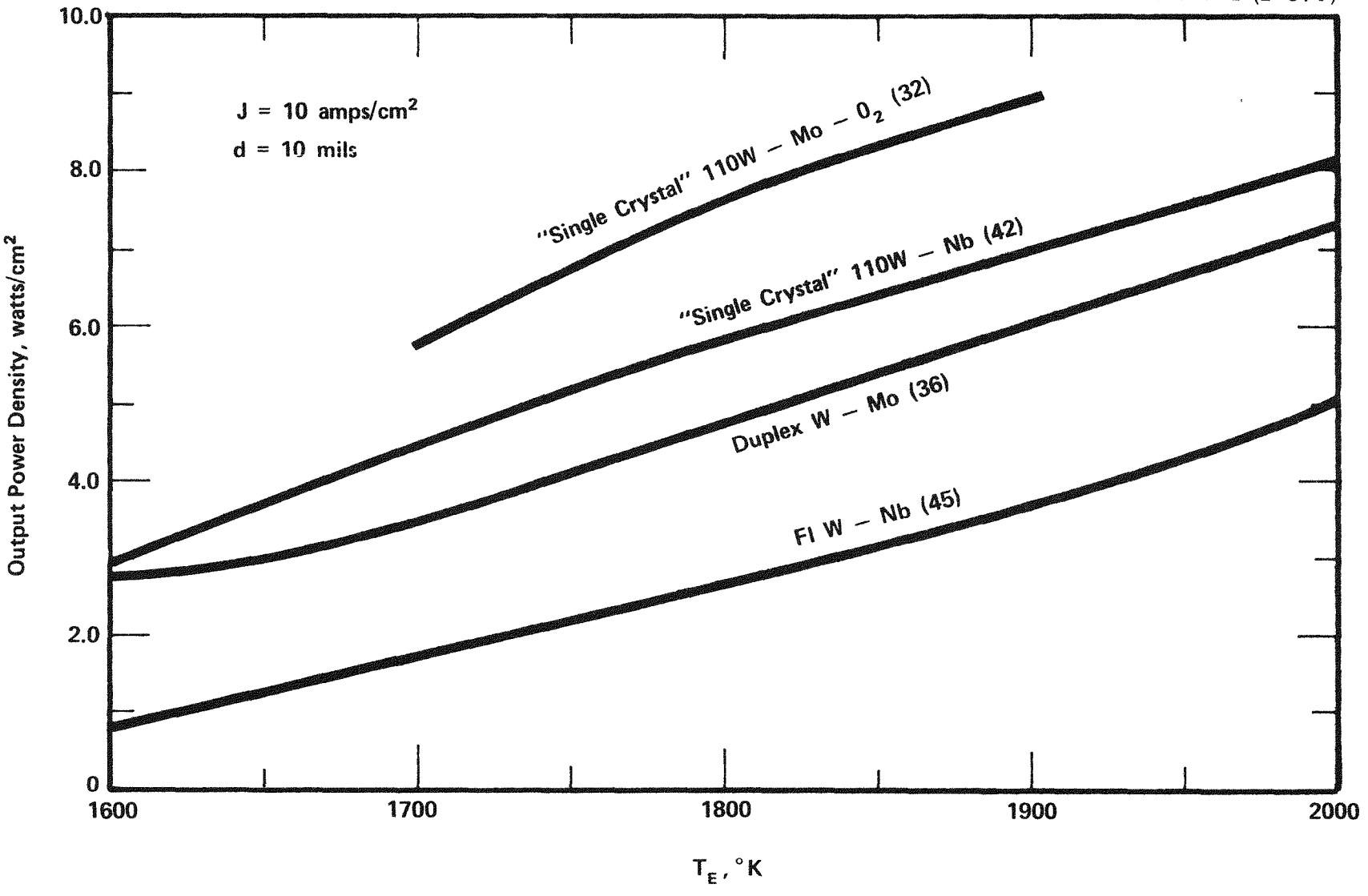

Figure 16. Performance Comparison of Several Emitters at Various Emitter Temperatures for J = 10 amps/cm and d = 10 mils.

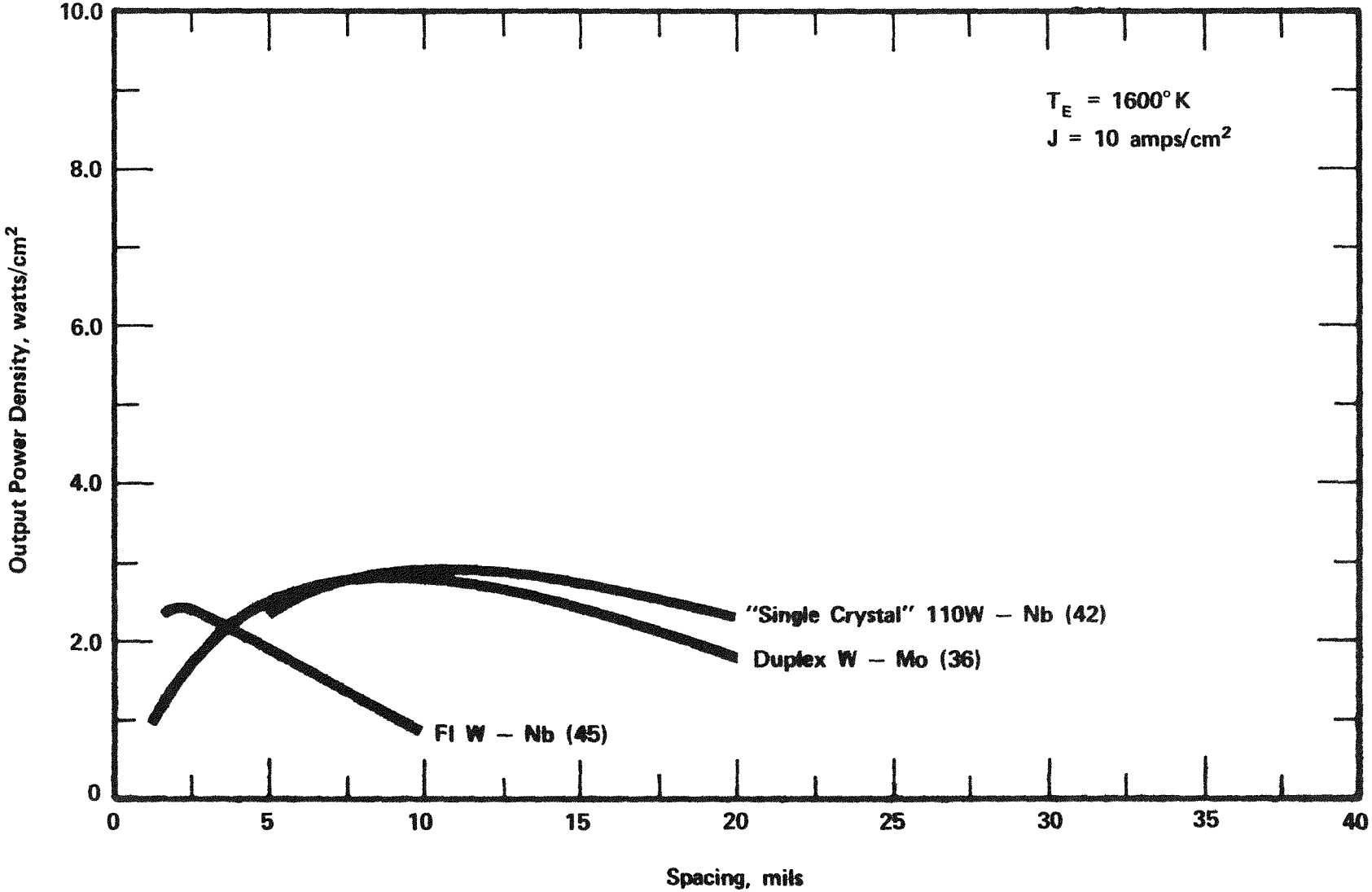

Figure 17. Performance Comparison of Several Emitters at Various Spacings for T_E = 1600°K and J = 10 amps/cm^2.

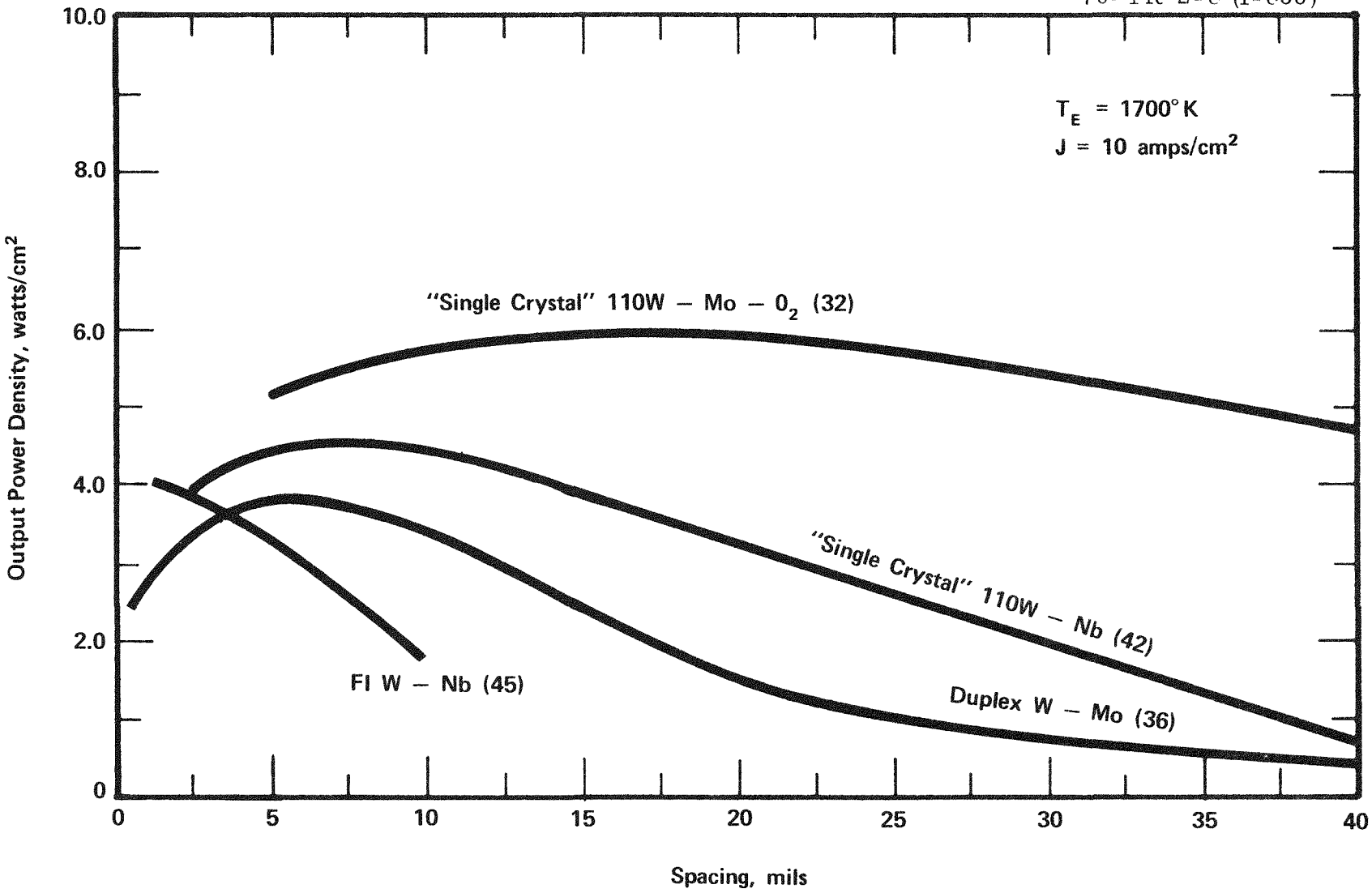

Figure 18. Performance Comparison of Several Emitters at Various Spacings for T_E = 1700°K and J = 10 amps/cm^2.

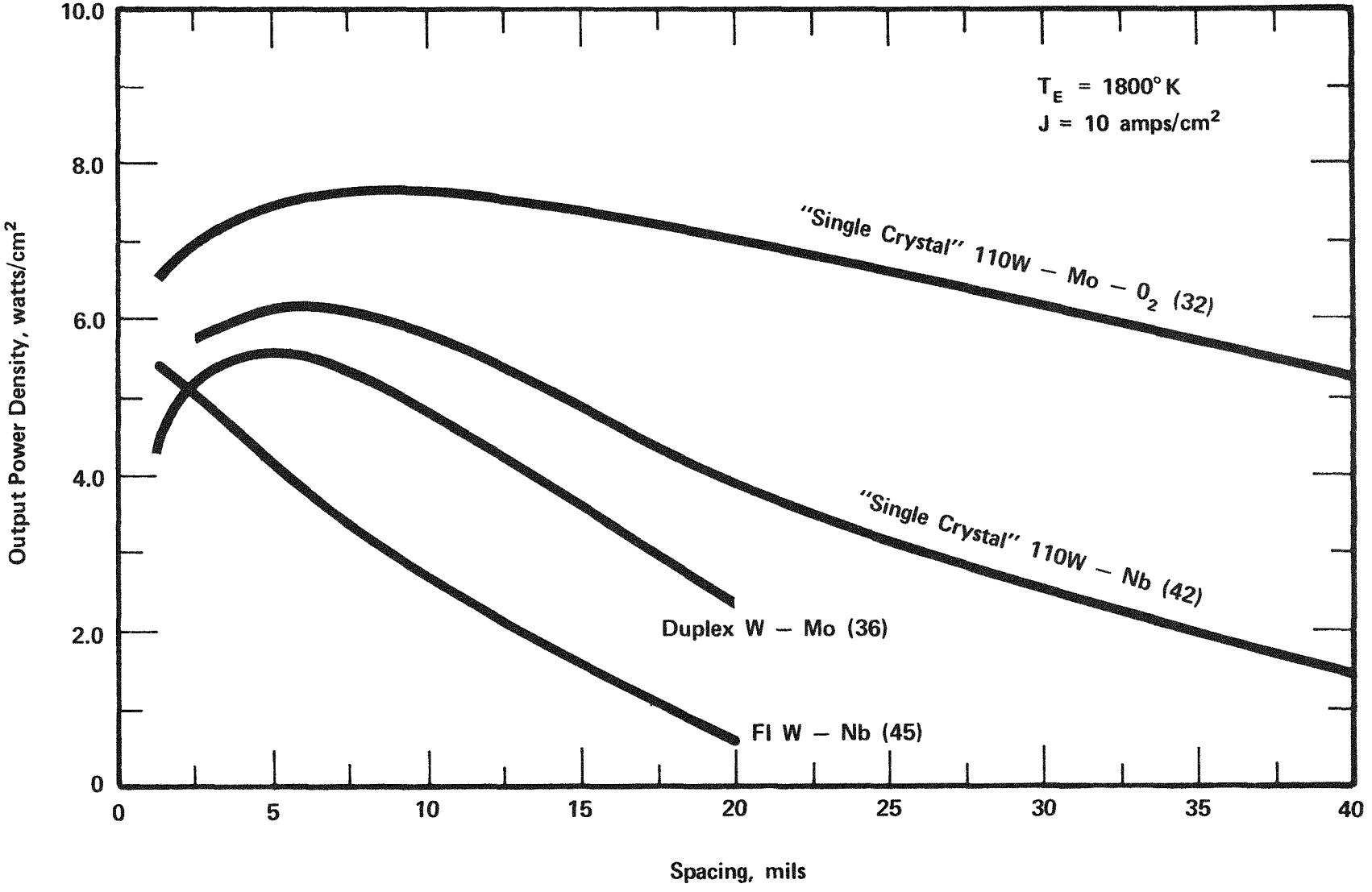

Figure 19. Performance Comparison of Several Emitters at Various Spacings for T_E = 1800°K and J = 10 amps/cm^2.

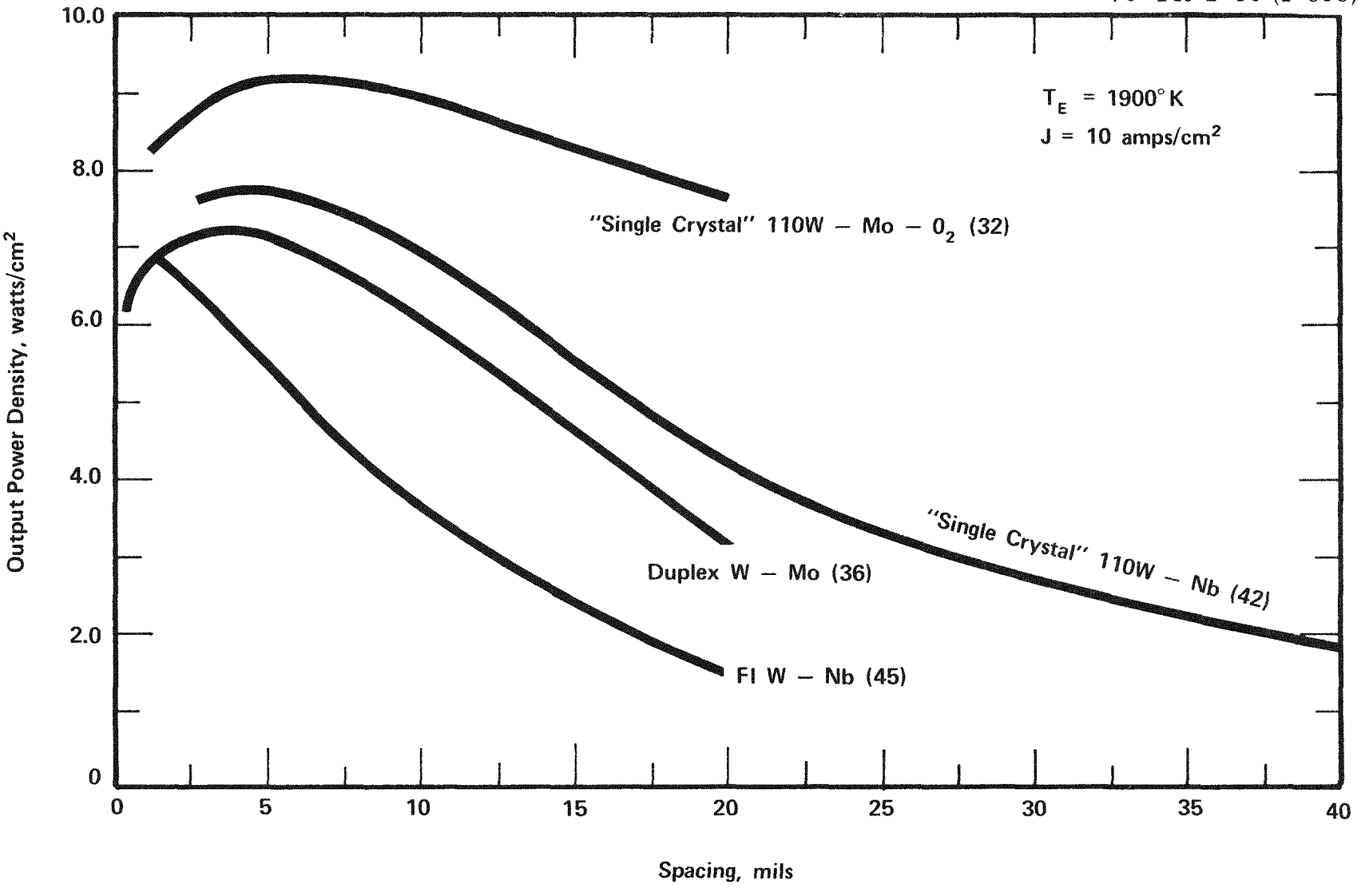

Figure 20. Performance Comparison of Several Emitters at Various Spacings for T_E = 1900°K and J = 10 amps/cm^2.

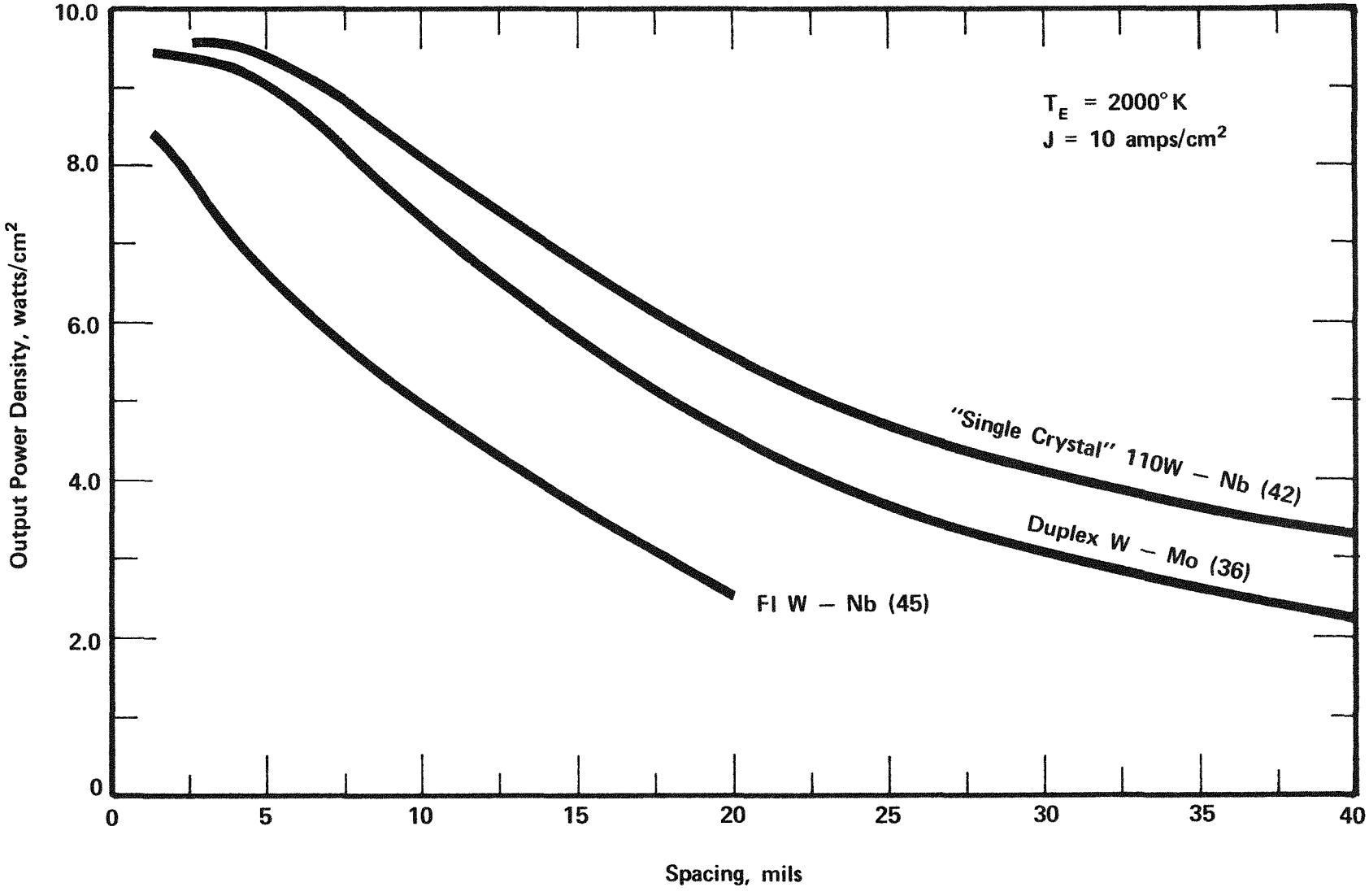

Figure 21. Performance Comparison of Several Emitters at Various Spacings for T_E = 2000°K and J = 10 amps/cm^2.

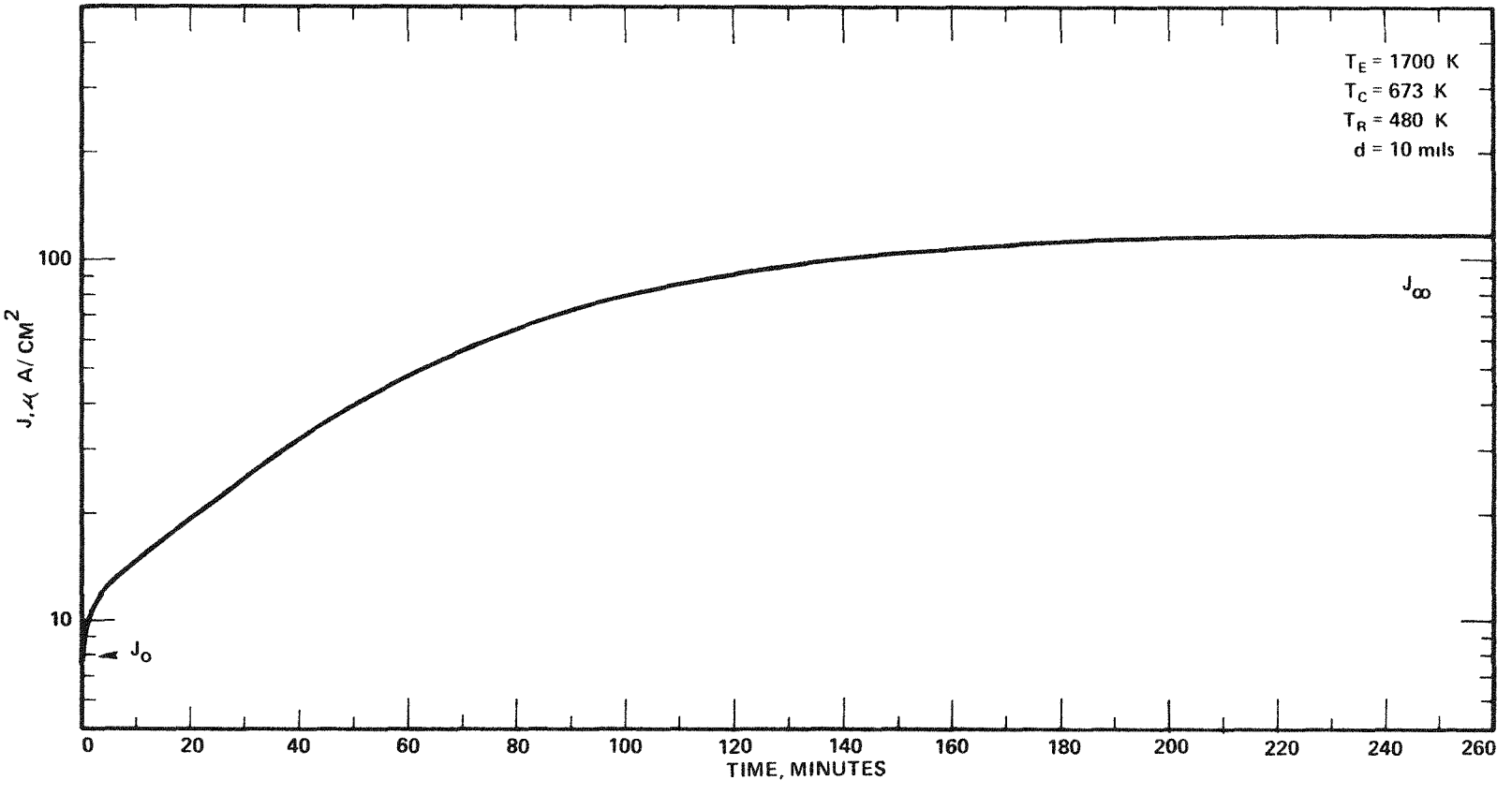

Figure 22. Time Dependence of Emission After a 10-minute Flash at 2000°K.

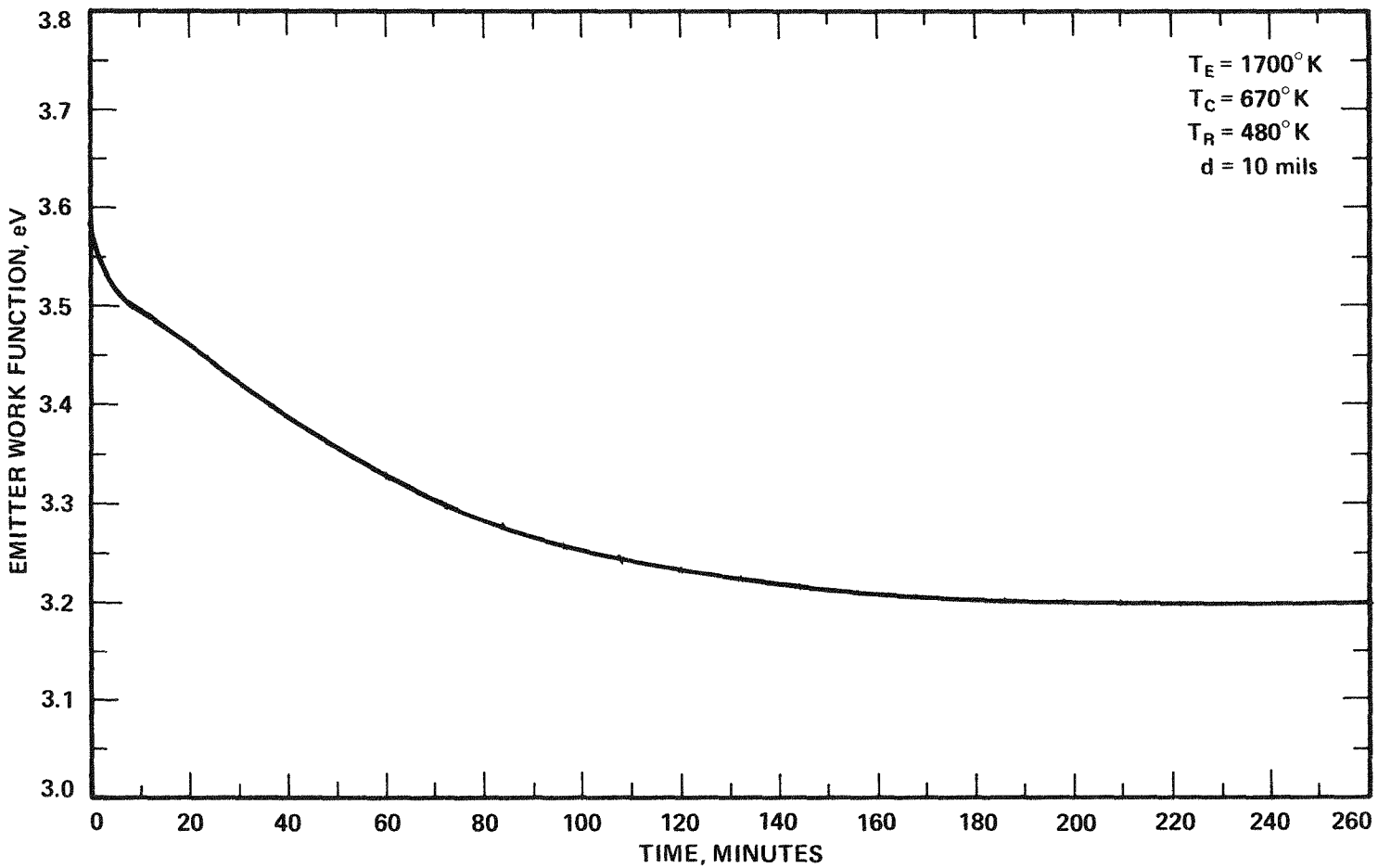

Figure 23. Time Dependence of Emitter Work Function After a 10-minute Flash at 2000°K.

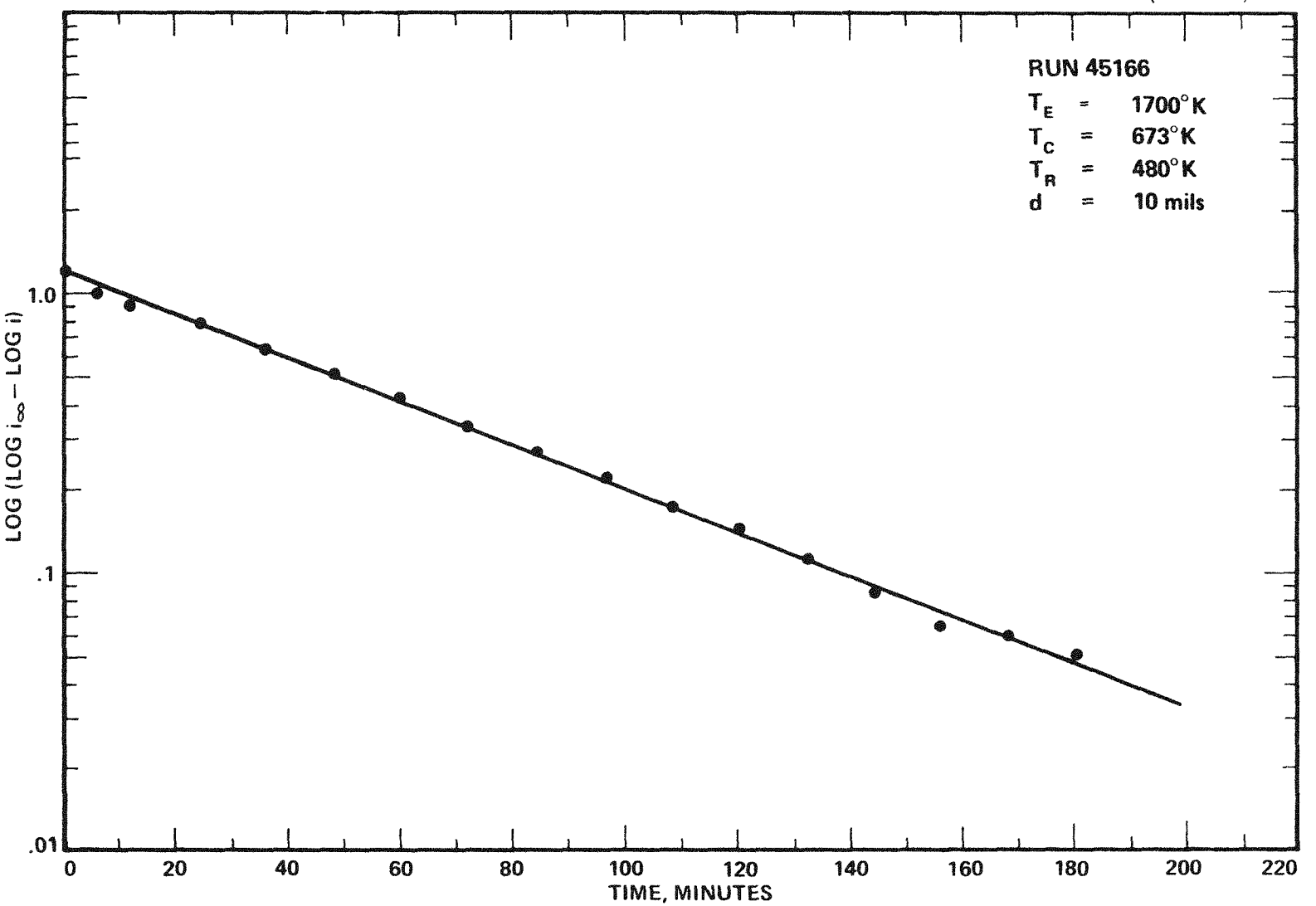

Figure 24. Presentation of the Data in Figure 23 According to Equation 9.

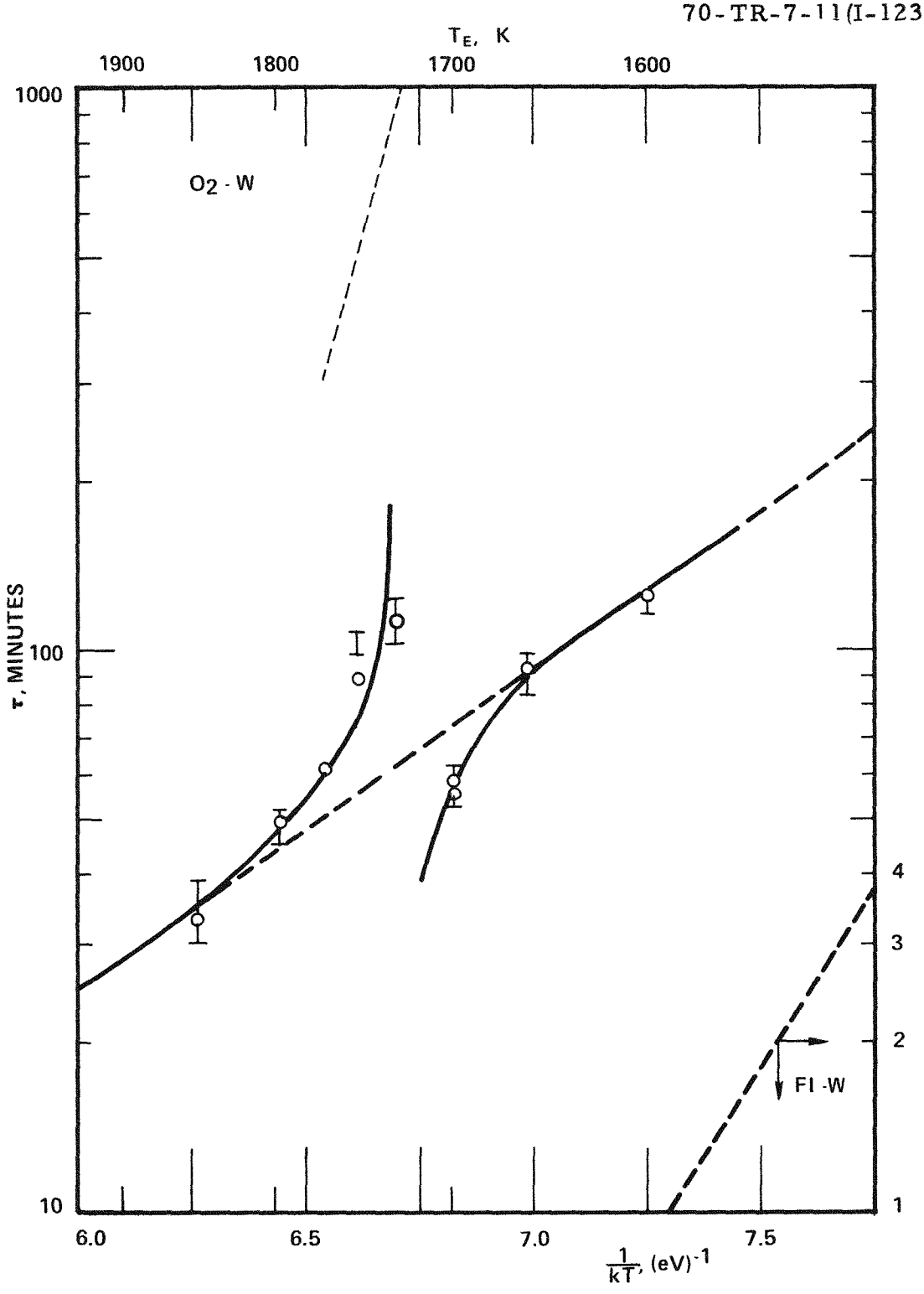

Figure 25. Evaporation Rate of the Additive from the Emitter Surface.

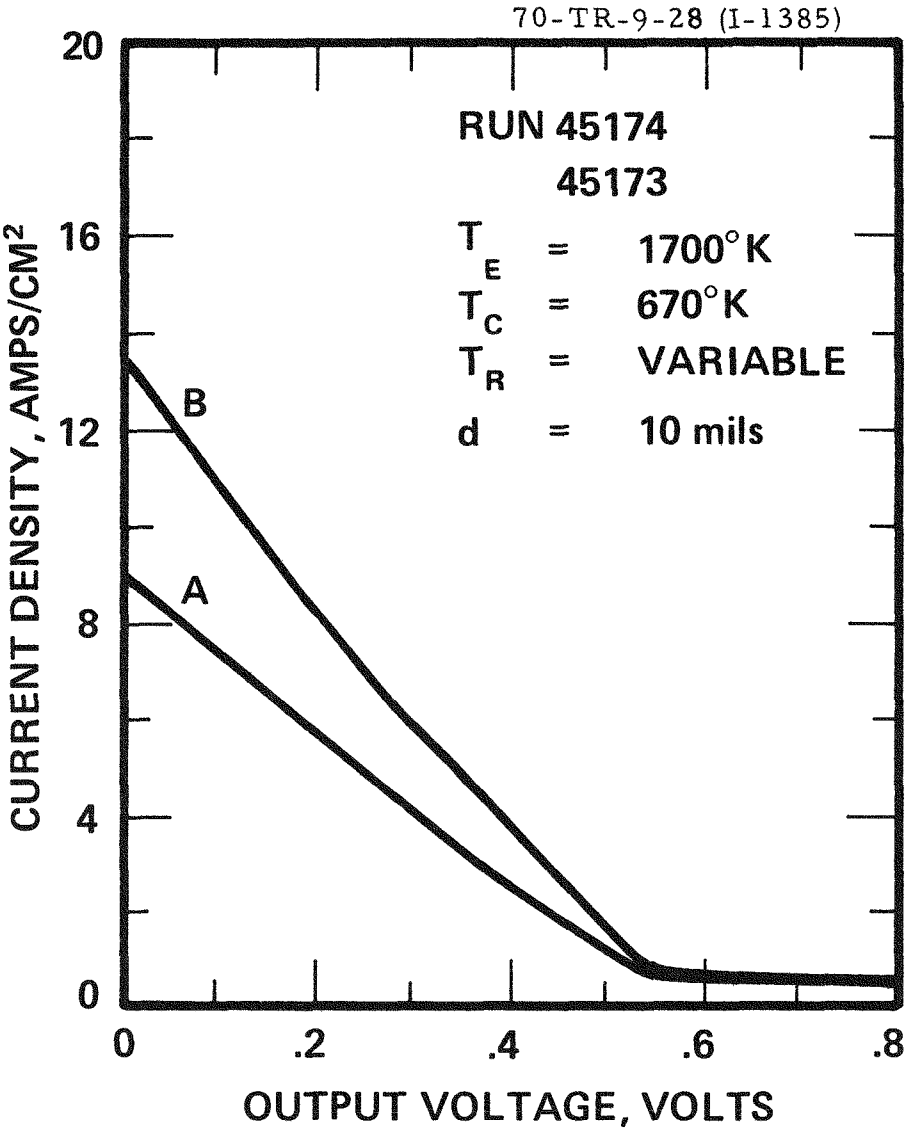

Figure 26. Comparison of the Performance Immediately After Flashing at 2000°K (curve A) with that 15 Hours After the Flash (curve B).

APPENDIX A
TEST CONVERTER

The test converter is a variable-parameter research-type device. It utilizes an active collector guard ring and a planar geometry The parameters whose values can be varied and accurately controlled include the emitter temperature, the interelectrode spacing, and the collector and reservoir temperatures. The active collector guard ring renders the conversion process free from any radial geometric dependence, and precisely defines the active area of the device The converter together with its supporting spacing mechanism and heaters is shown in a schematic drawing in Figure A-1 and in a photograph in Figure A-2. The converter itself is shown in Figure A-3.

The emitter is mounted above the collector assembly and has a sleeve extending away from the collector This arrangement greatly reduces stray effects due to sleeve emission. A niobium shield surrounding the sleeve further reduces the stray emission currents while at the same time it serves as a getter and provides thermal protection for the spacing bellows. The emitter is heated by electron bombardment from a filament mounted inside the emitter sleeve, while a tantalum shield on the electron gun keeps the sleeve from being bombarded. A hohlraum in the rear face of the emitter is used for temperature measurement. Several additional holes are provided for thermocouple or photocell temperature measurement and control

The collector-guard assembly is fabricated from molybdenum but provides for different electrode materials through the use of brazed-in plates in the active converter region. A sapphire spacing ring determines the vertical distance between the guard and collector electrode surfaces A value of 1 - 1.5 mil is established during machining The radial alignment is maintained by a series of sapphire balls retained in a groove

just below the collector face. The radial spacing is about 4 mils. A pair of thermocouple holes in the guard is used for temperature control. In the collector, there are three sets of holes which provide additional heat flux measurement capabilities. The active area of the collector is 2 cm^2, while that of the emitter is 3 cm^2. A collector guard assembly is shown in Figure A-4.

The flexible nickel bellows is partially welded together before being brazed to the emitter and collector subassemblies. The final diode closure is made by electron beam welding the emitter section bellows flange to that of the collector section. There is sufficient flexibility to allow spacing excursions from 0 to 100 mil. The collector and guard heater-coolers are maintained in good thermal contact with the collector and guard structures by spring-loading on the tapered mating surfaces. The design allows the electrode temperatures to be controlled with both high and low current static loading.

Cesium pressure in the converter is controlled from a liquid reservoir connected to the active region by a tube on the mounting plate for the emitter sleeve. The reservoir is electrically heated and water cooled to give a fast response when the temperature must be changed. The heater-cooler is arranged to maintain the temperature gradients in the liquid to less than 1°K.

Interelectrode spacing is adjusted by varying the distance between the emitter ring and the guard support plate. The spring loading on the heater-coolers also serves to maintain solid contact between the rigidly mounted guard locating plate and the guard surface. Three micrometers, mounted on the water-cooled emitter support plate, are extended to the guard locating plate through three ceramic

rods. The micrometer control shafts are brought through the top plate of the vacuum bell jar to allow spacing adjustment during converter operation. A gear box on the outside of the bell jar provides either separate or combined control of the micrometers. Spacing changes may be read directly from the micrometers and a zero reference is established by momentarily shorting the converter. The electrodes can be set and maintained parallel within 0.3 mils at the emitter edge, and the spacing mechanism has a precision of 0.2 mils. Minimum spacing is typically 0.2 - 0.5 mil but tends to increase each time the device is shorted and material is pulled from the collector. Usually a minimum is determined for each emitter temperature during initial testing and this value is used for all further experiments.

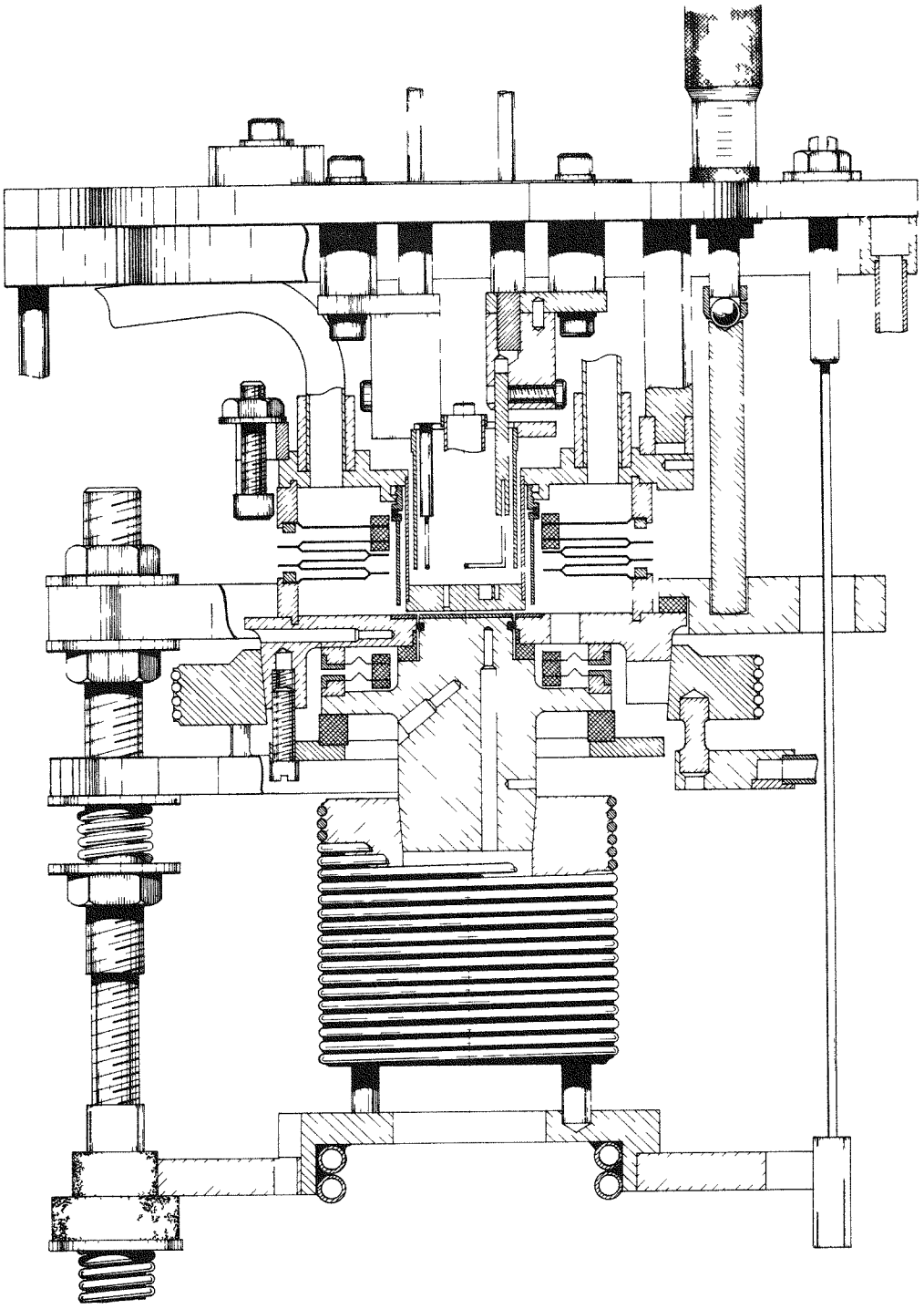

Figure A-1. Research Variable Parameter Converter.

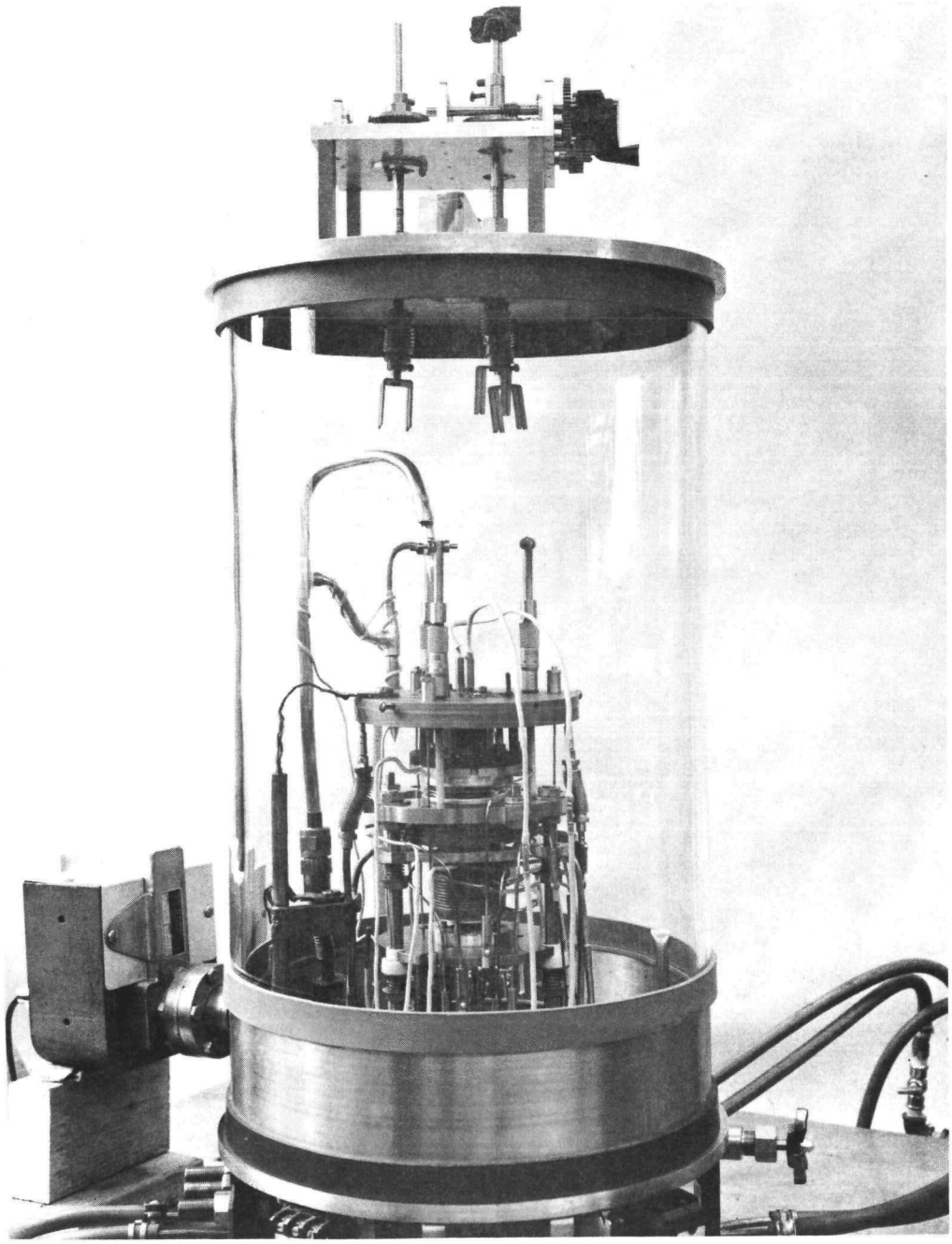

Figure A-2. Variable Parameter Converter, Ready for Outgassing.

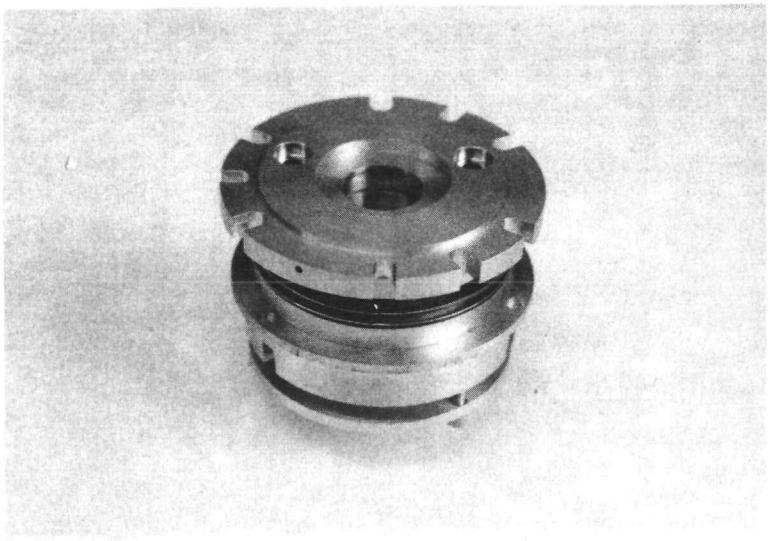

Figure -3. Variable Parameter Converter without Tubulation.

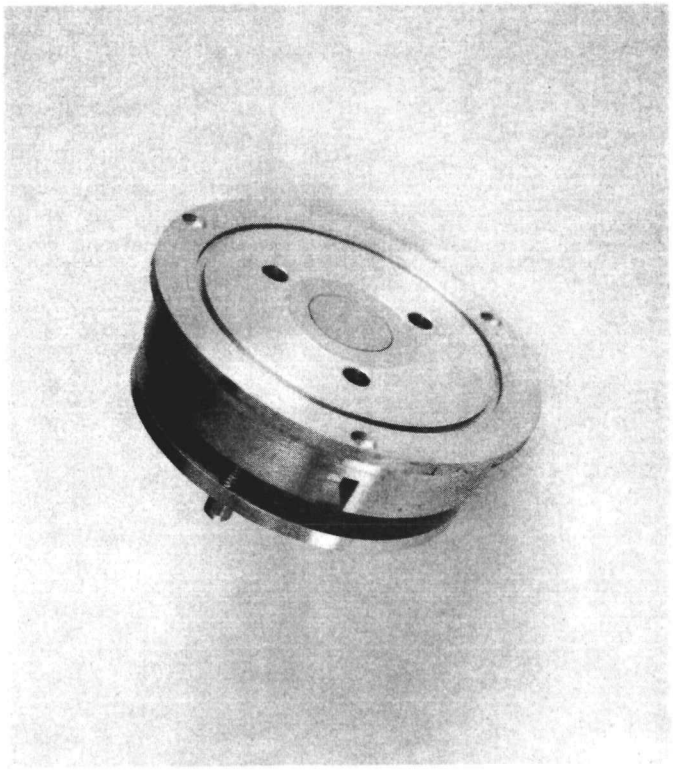

Figure A-4. Collector Guard Subassembly.

APPENDIX B

FAMILIES OF VOLT-AMPERE CHARACTERISTICS

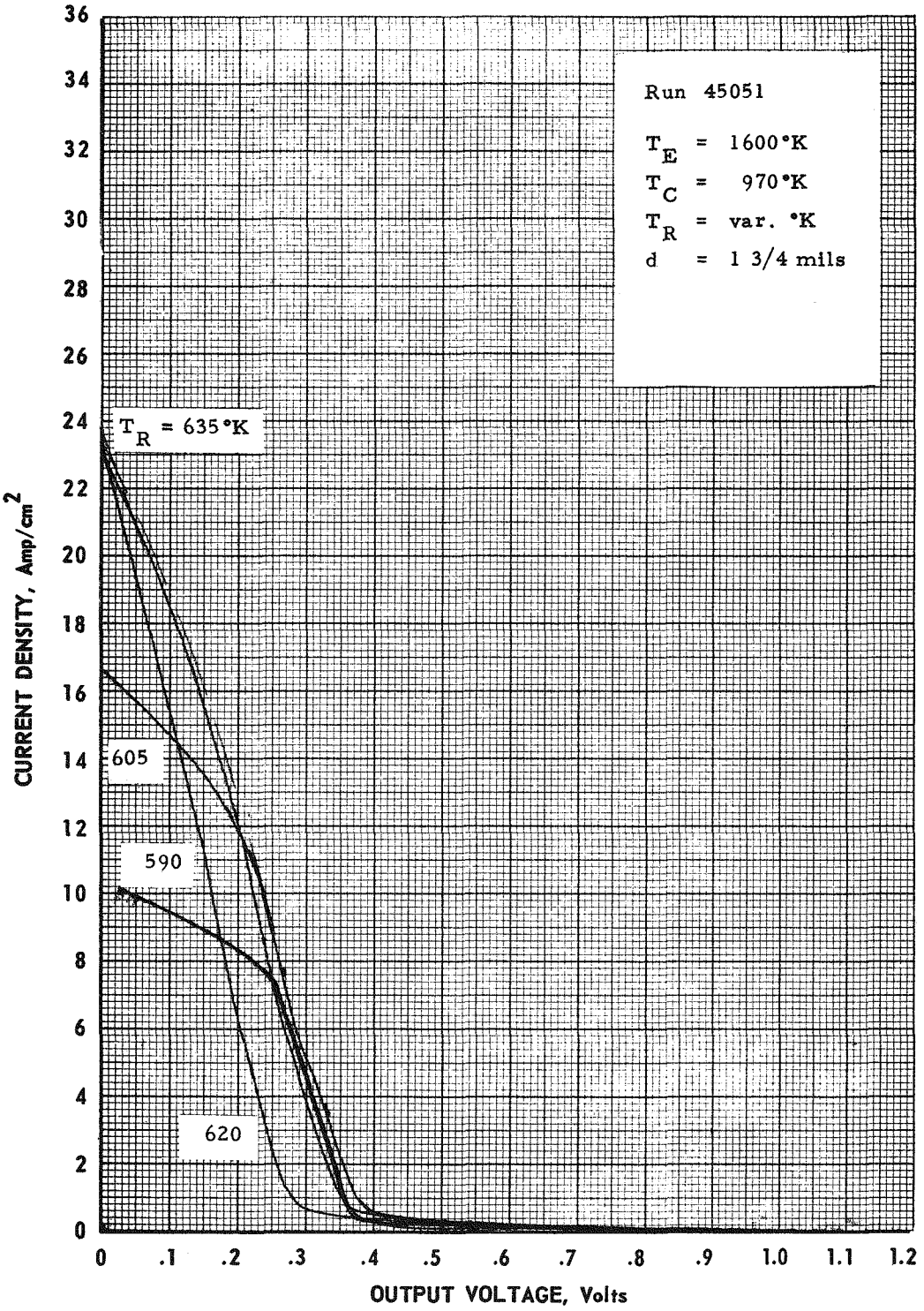
Run 45051
T_E = 1600°K
T_C = 970°K
T_R = var. °K
d = 1 3/4 mils
T_R = 635°K
605
590
620
CURRENT DENSITY, Amp/cm^2
OUTPUT VOLTAGE, Volts
0
2
4
6
8
10
12
14
16
18
20
22
24
26
28
30
32
34
36
0
.1
.2
.3
.4
.5
.6
.7
.8
.9
1.0
1.1
1.2

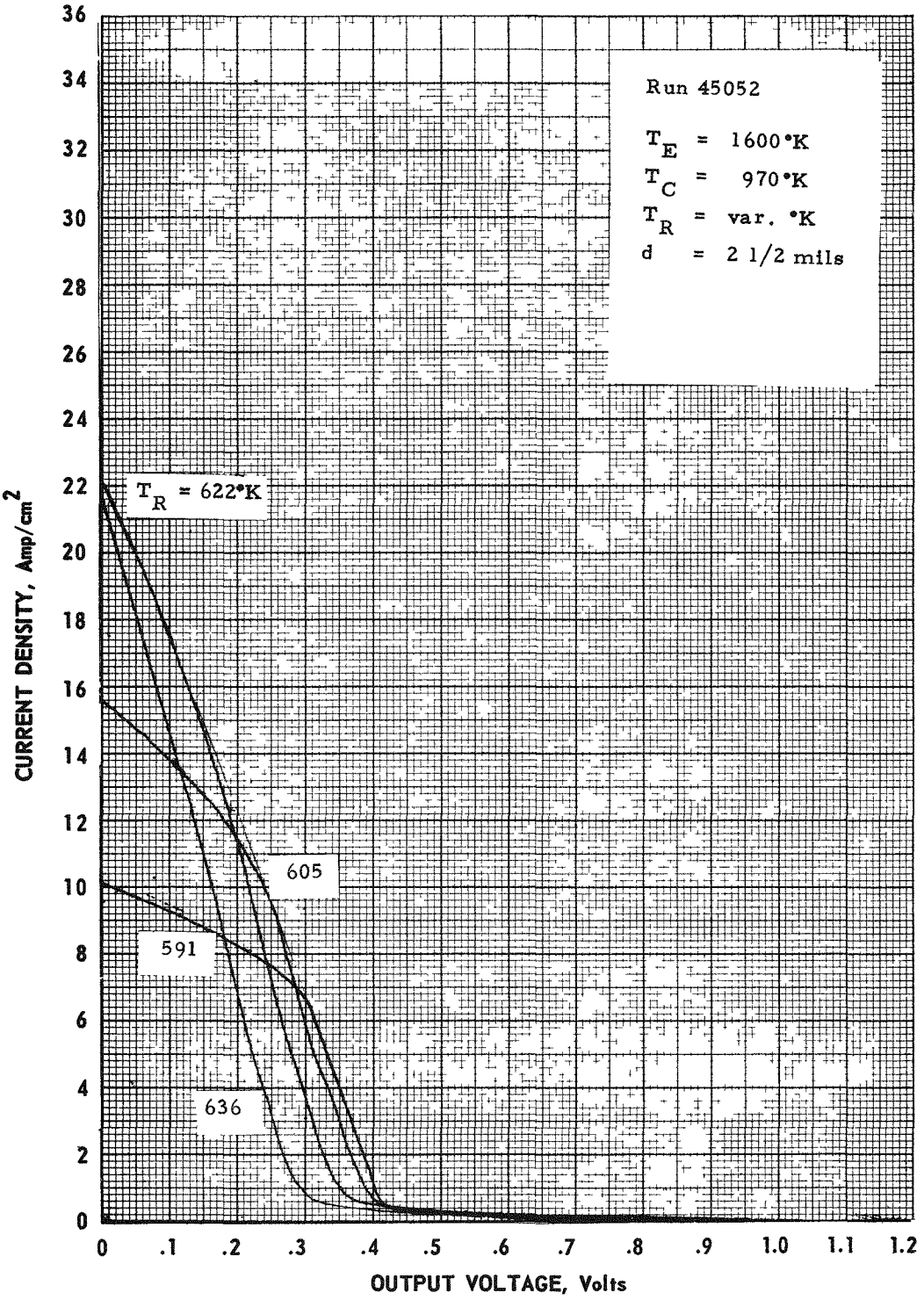
Run 45052
T_E = 1600°K
T_C = 970°K
T_R = var. °K
d = 2 1/2 mils
T_R = 622°K
605
591
636
CURRENT DENSITY, Amp/cm^2
OUTPUT VOLTAGE, Volts
0
2
4
6
8
10
12
14
16
18
20
22
24
26
28
30
32
34
36
0
.1
.2
.3
.4
.5
.6
.7
.8
.9
1.0
1.1
1.2

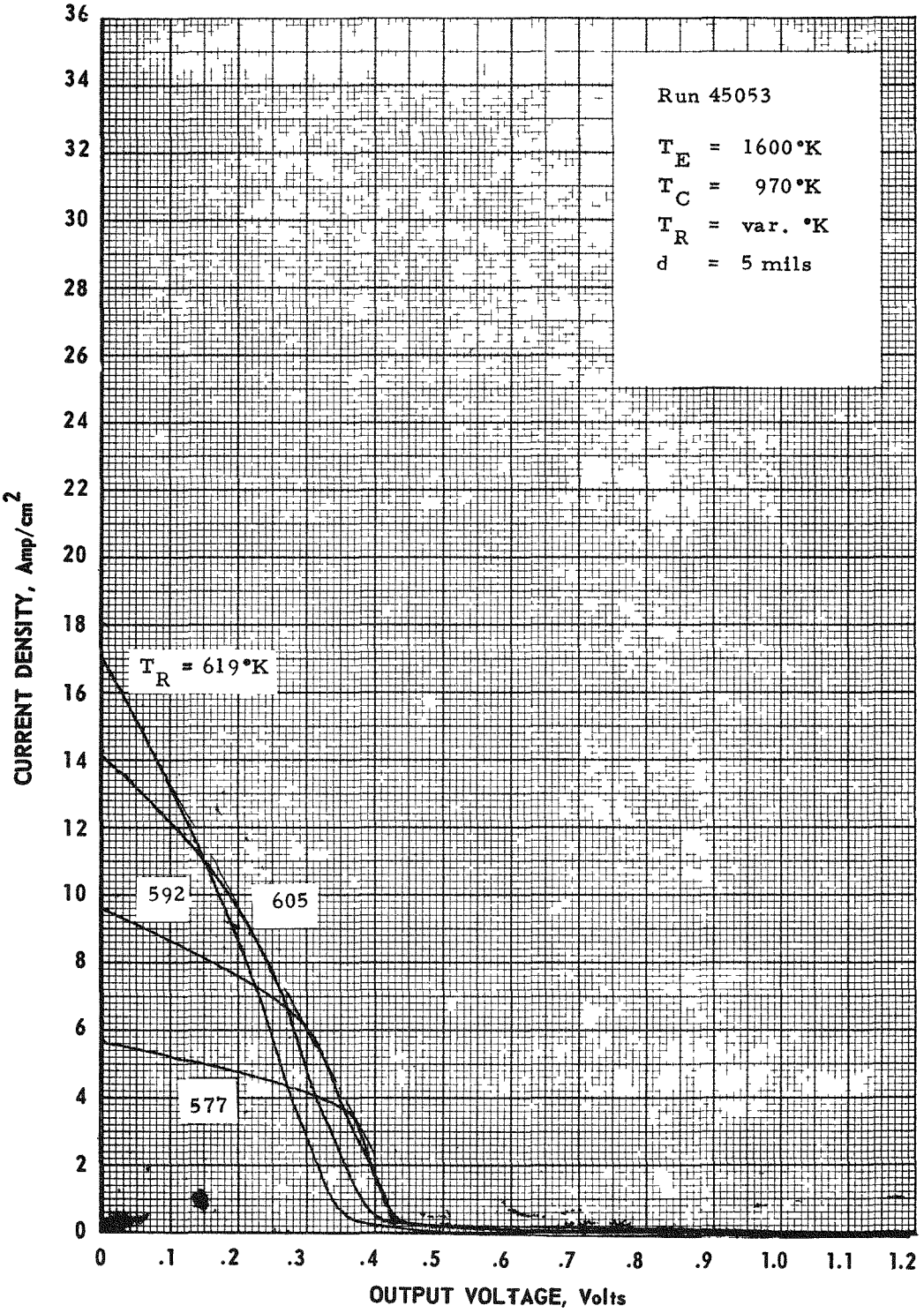
Run 45053
T_E = 1600°K
T_C = 970°K
T_R = var. °K
d = 5 mils
T_R = 619°K
592
605
577
CURRENT DENSITY, Amp/cm^2
OUTPUT VOLTAGE, Volts
0
2
4
6
8
10
12
14
16
18
20
22
24
26
28
30
32
34
36
0
.1
.2
.3
.4
.5
.6
.7
.8
.9
1.0
1.1
1.2

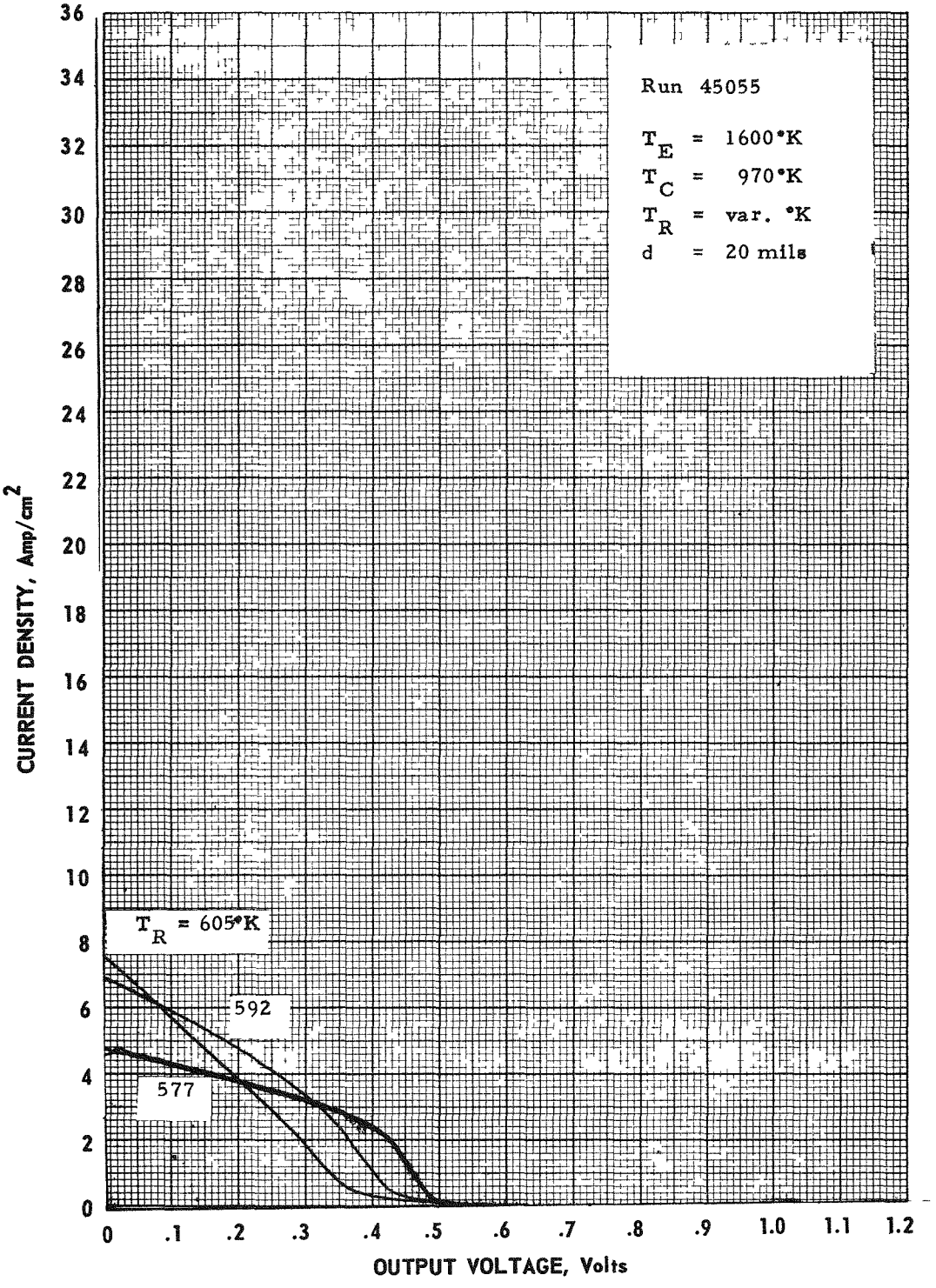
Run 45055
T_E = 1600°K
T_C = 970°K
T_R = var. °K
d = 20 mils
T_R = 605°K
592
577
CURRENT DENSITY, Amp/cm^2
OUTPUT VOLTAGE, Volts
0
2
4
6
8
10
12
14
16
18
20
22
24
26
28
30
32
34
36
0
.1
.2
.3
.4
.5
.6
.7
.8
.9
1.0
1.1
1.2

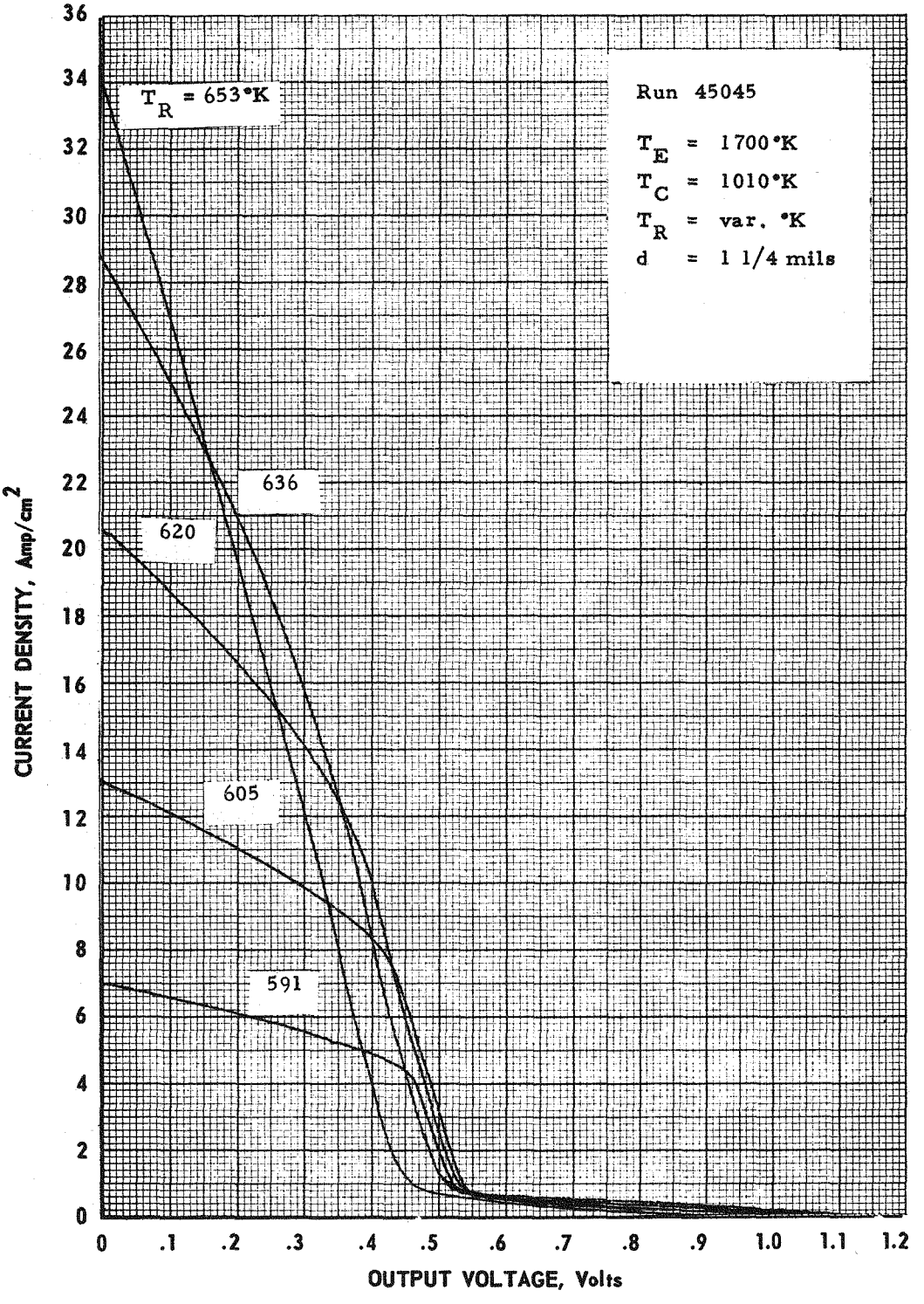
Run 45045
T_E = 1700°K
T_C = 1010°K
T_R = var. °K
d = 1 1/4 mils
T_R = 653°K
636
620
605
591
CURRENT DENSITY, Amp/cm^2
OUTPUT VOLTAGE, Volts
0
2
4
6
8
10
12
14
16
18
20
22
24
26
28
30
32
34
36
0
.1
.2
.3
.4
.5
.6
.7
.8
.9
1.0
1.1
1.2

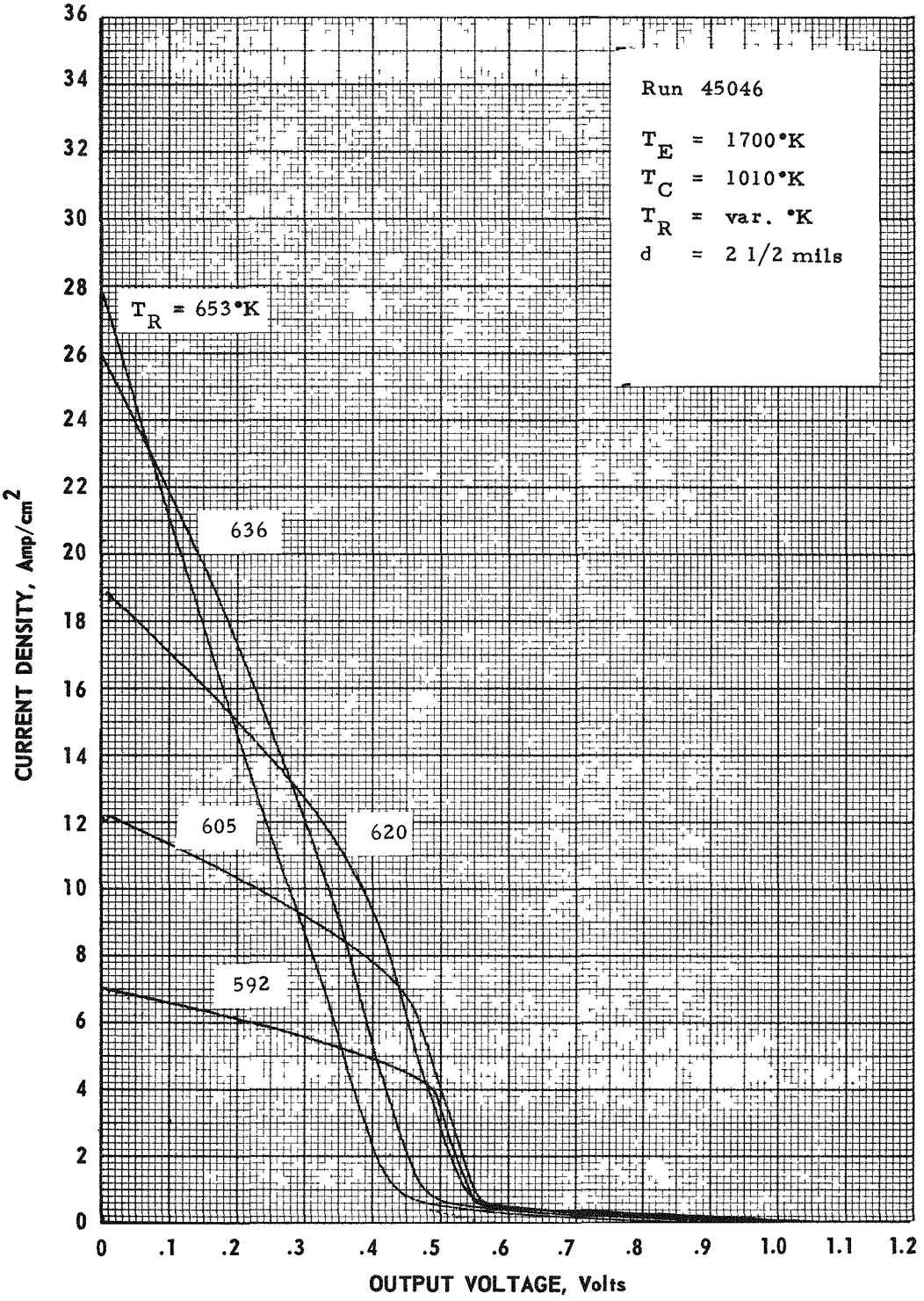
Run 45046
T_E = 1700°K
T_C = 1010°K
T_R = var. °K
d = 2 1/2 mils
T_R = 653°K
636
620
605
592
CURRENT DENSITY, Amp/cm^2
OUTPUT VOLTAGE, Volts
0
2
4
6
8
10
12
14
16
18
20
22
24
26
28
30
32
34
36
0
.1
.2
.3
.4
.5
.6
.7
.8
.9
1.0
1.1
1.2

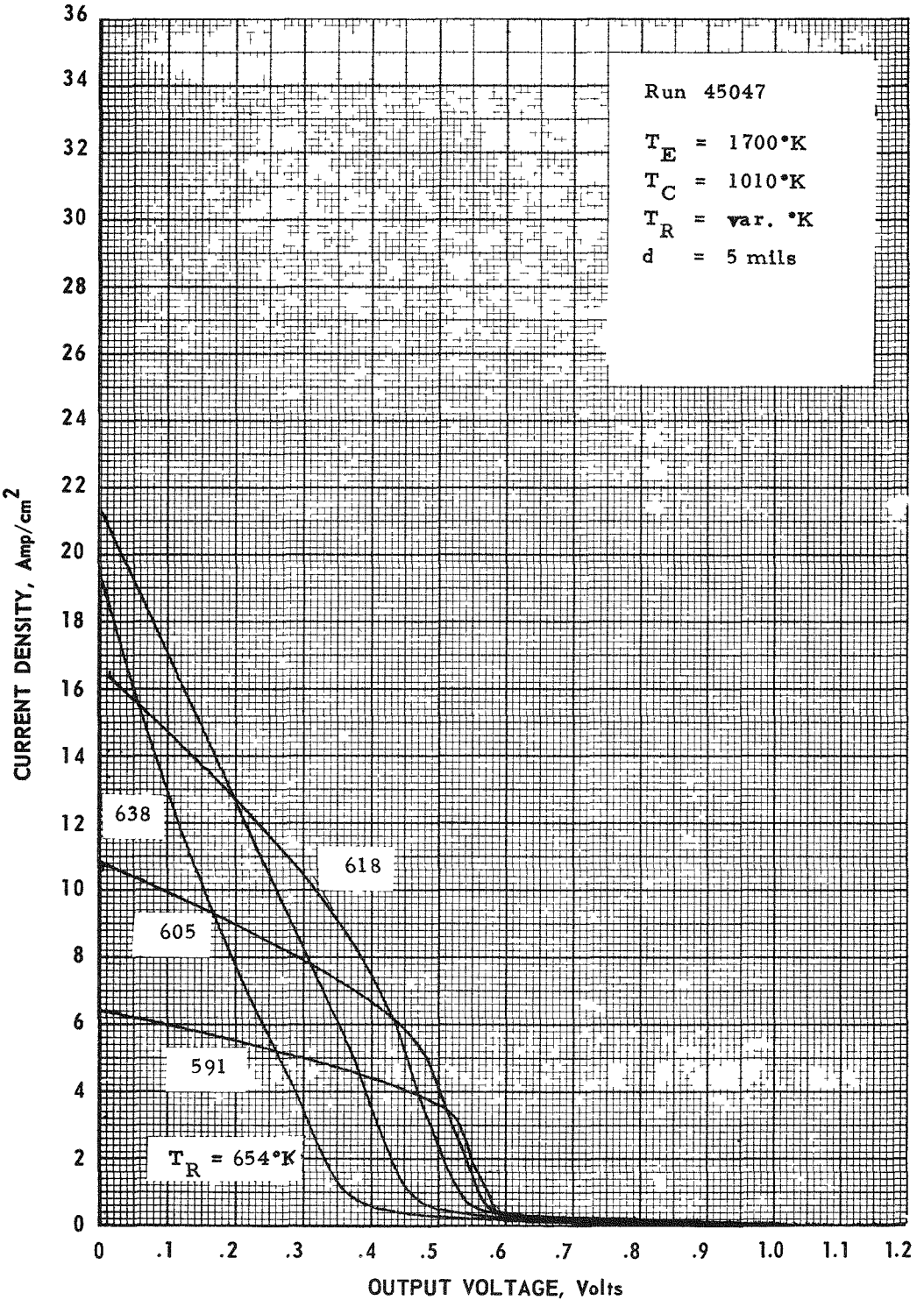
Run 45047
T_E = 1700°K
T_C = 1010°K
T_R = var. °K
d = 5 mils
638
618
605
591
T_R = 654°K
CURRENT DENSITY, Amp/cm^2
OUTPUT VOLTAGE, Volts
0
2
4
6
8
10
12
14
16
18
20
22
24
26
28
30
32
34
36
0
.1
.2
.3
.4
.5
.6
.7
.8
.9
1.0
1.1
1.2

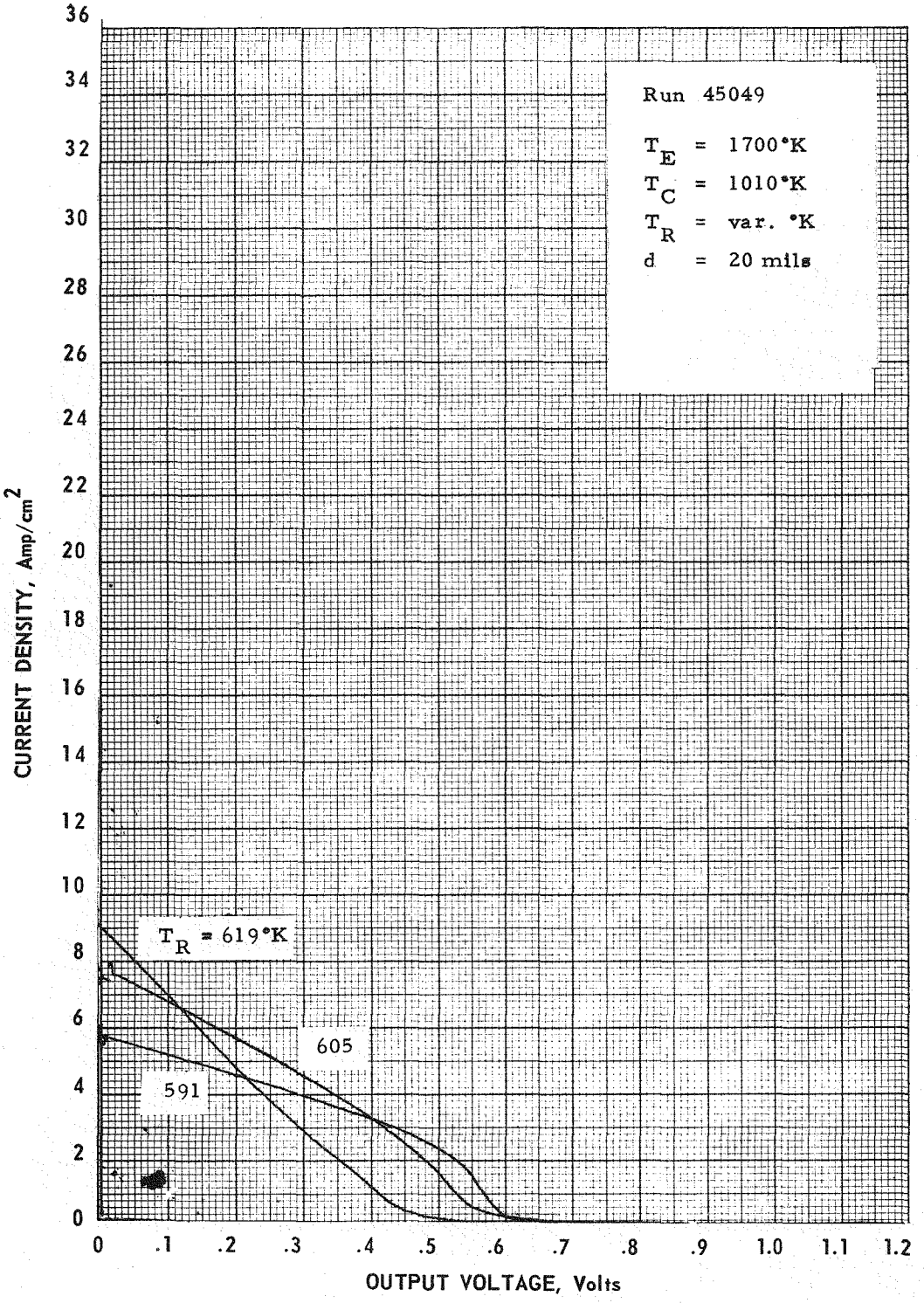
Run 45049
T_E = 1700°K
T_C = 1010°K
T_R = var. °K
d = 20 mils
T_R = 619°K
605
591
CURRENT DENSITY, Amp/cm^2
OUTPUT VOLTAGE, Volts
0
2
4
6
8
10
12
14
16
18
20
22
24
26
28
30
32
34
36
0
.1
.2
.3
.4
.5
.6
.7
.8
.9
1.0
1.1
1.2

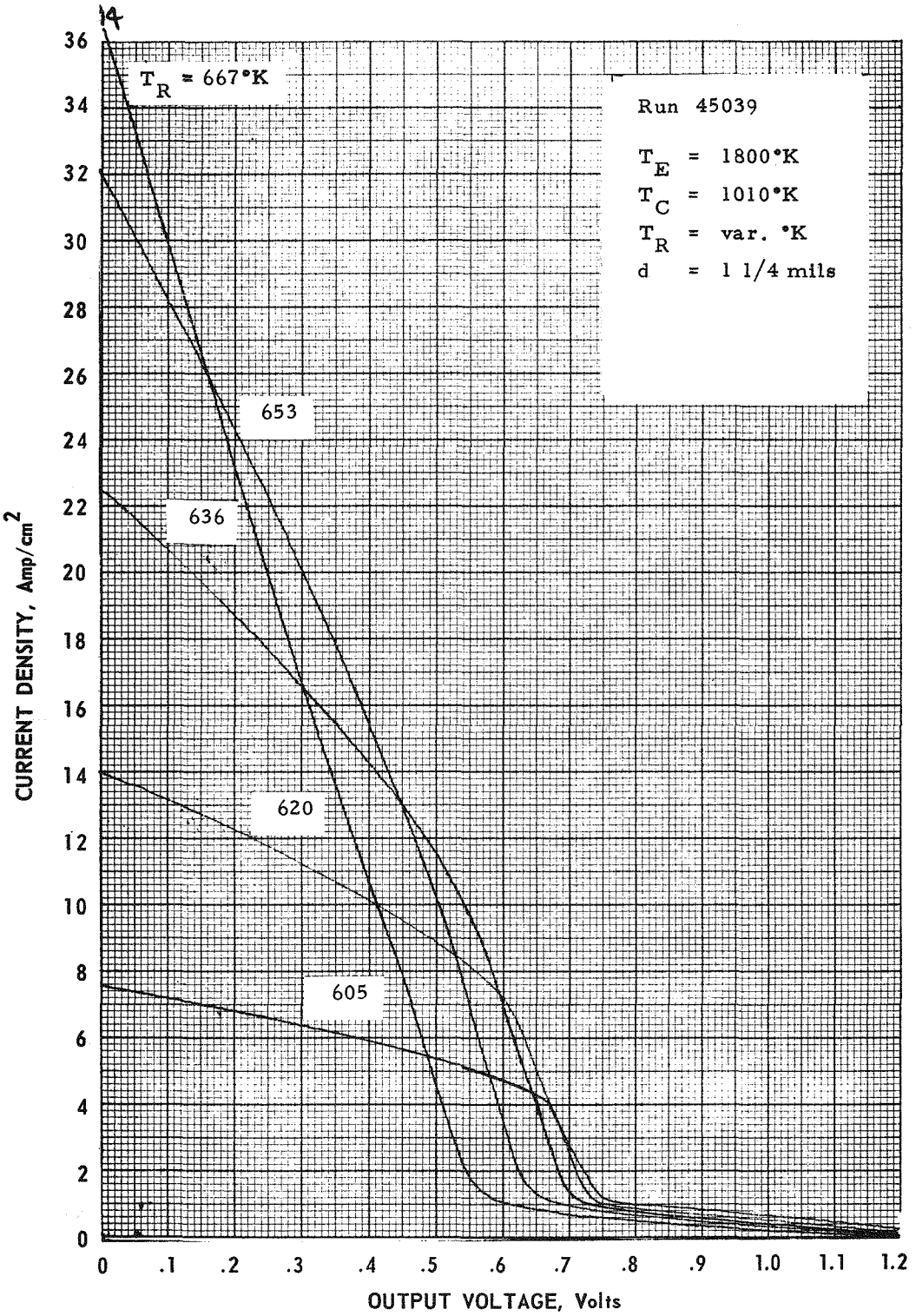
14
T_R = 667°K
Run 45039
T_E = 1800°K
T_C = 1010°K
T_R = var. °K
d = 1 1/4 mils
653
636
620
605
CURRENT DENSITY, Amp/cm^2
OUTPUT VOLTAGE, Volts
0
2
4
6
8
10
12
14
16
18
20
22
24
26
28
30
32
34
36
0
.1
.2
.3
.4
.5
.6
.7
.8
.9
1.0
1.1
1.2

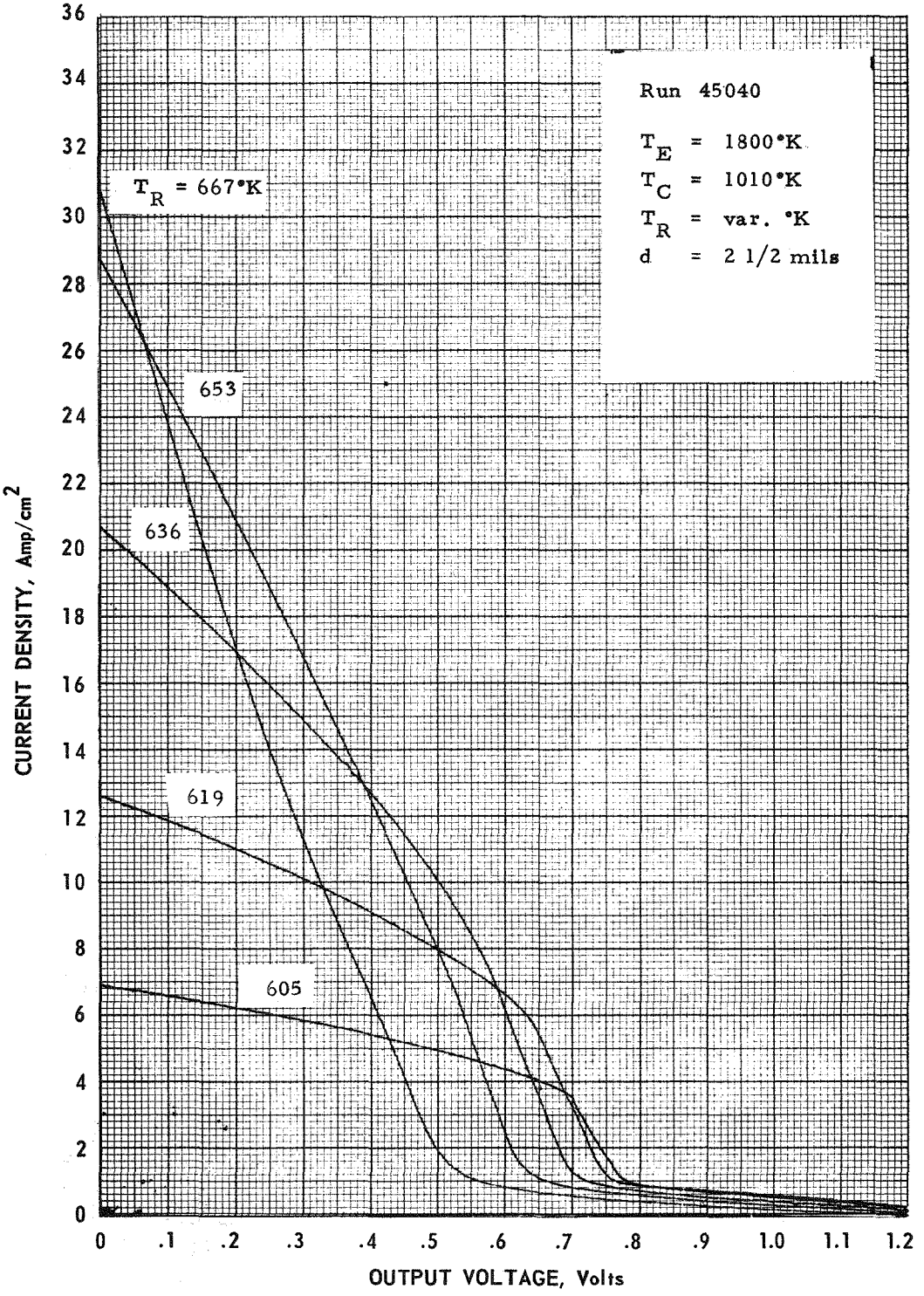
Run 45040
T_E = 1800°K
T_C = 1010°K
T_R = var. °K
d = 2 1/2 mils
T_R = 667°K
653
636
619
605
CURRENT DENSITY, Amp/cm^2
OUTPUT VOLTAGE, Volts
0
2
4
6
8
10
12
14
16
18
20
22
24
26
28
30
32
34
36
0
.1
.2
.3
.4
.5
.6
.7
.8
.9
1.0
1.1
1.2

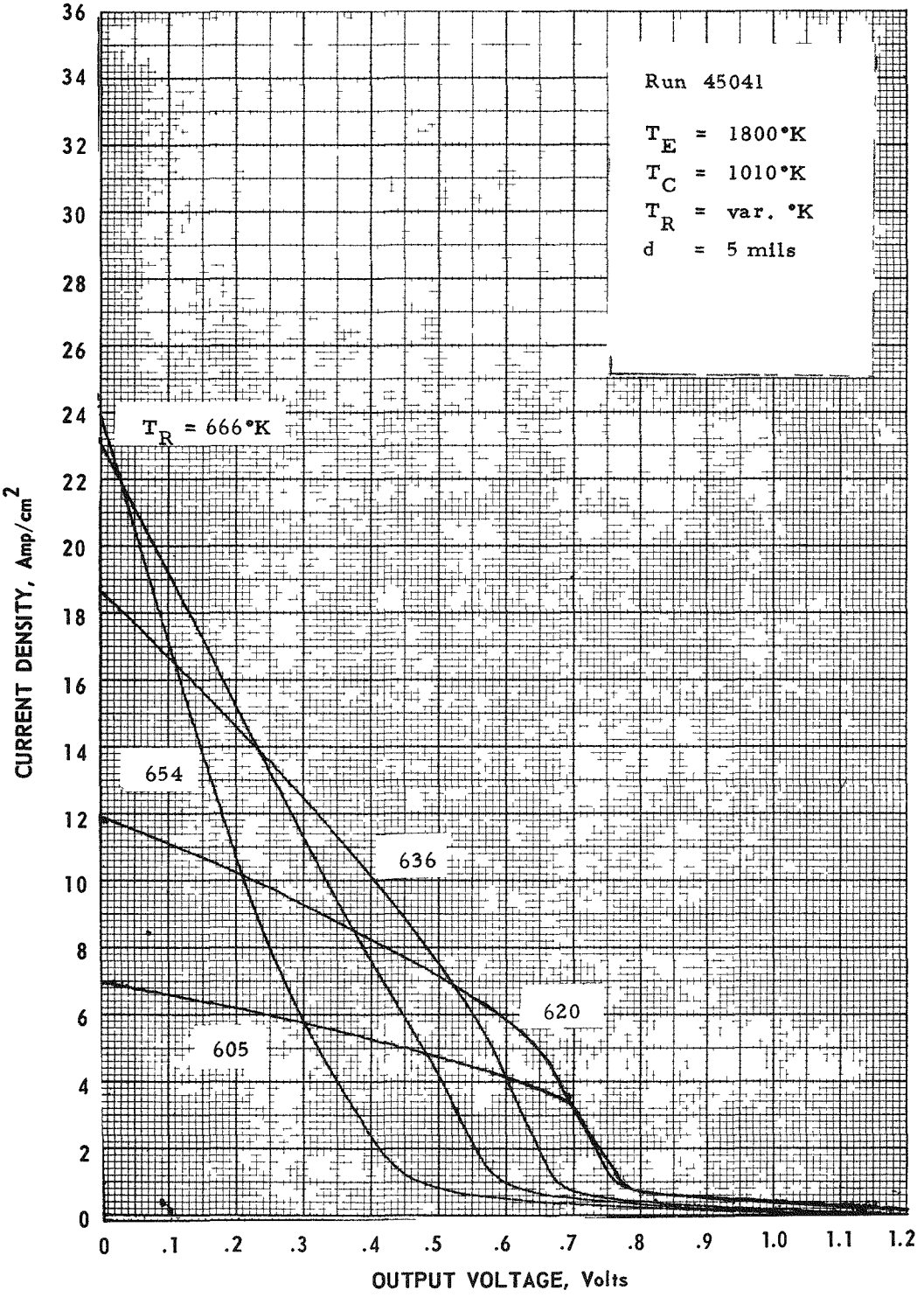
Run 45041
T_E = 1800°K
T_C = 1010°K
T_R = var. °K
d = 5 mils
T_R = 666°K
654
636
620
605
CURRENT DENSITY, Amp/cm^2
OUTPUT VOLTAGE, Volts
0
2
4
6
8
10
12
14
16
18
20
22
24
26
28
30
32
34
36
0
.1
.2
.3
.4
.5
.6
.7
.8
.9
1.0
1.1
1.2

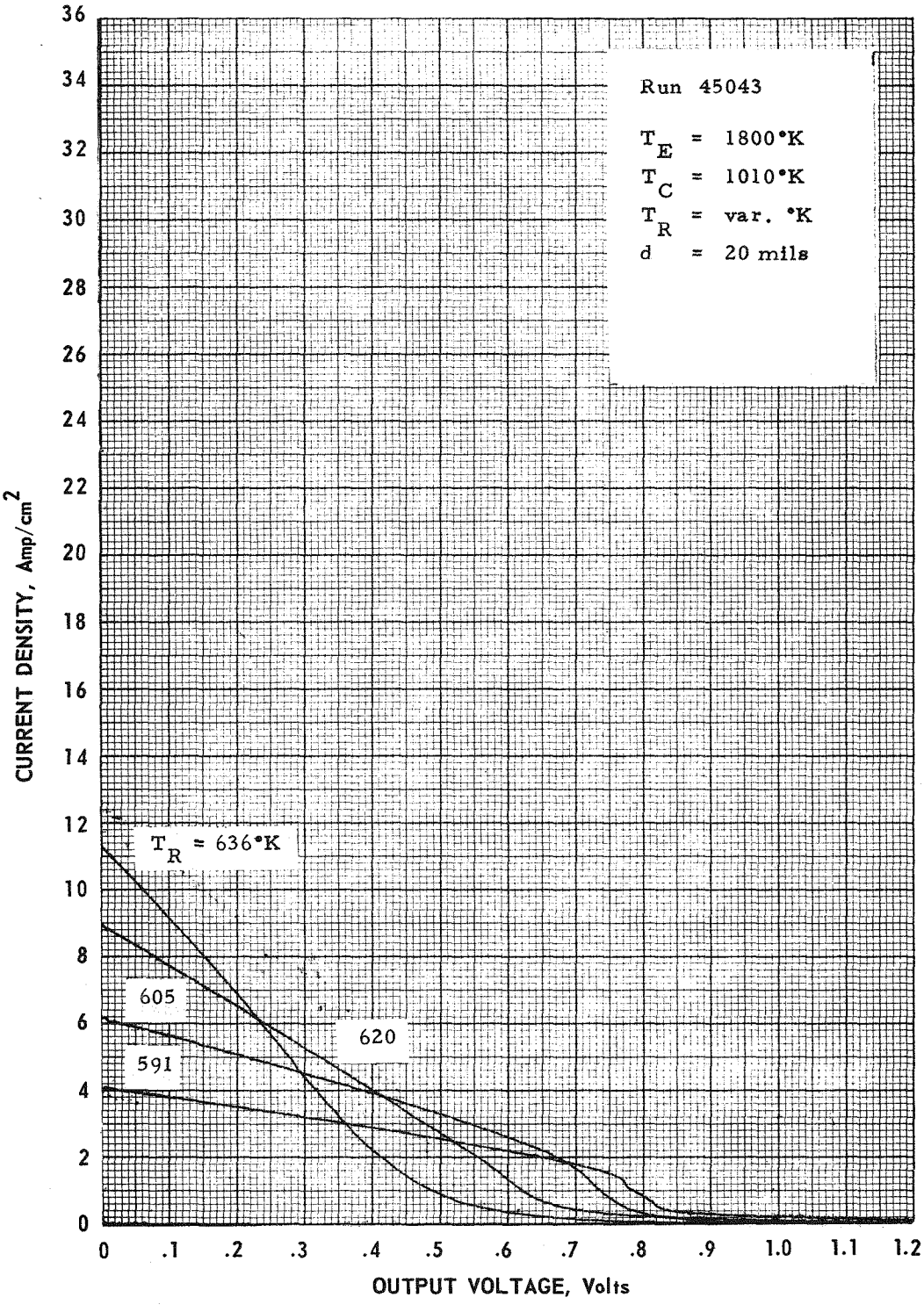
Run 45043
T_E = 1800°K
T_C = 1010°K
T_R = var. °K
d = 20 mils
T_R = 636°K
605
620
591
CURRENT DENSITY, Amp/cm^2
OUTPUT VOLTAGE, Volts
0
2
4
6
8
10
12
14
16
18
20
22
24
26
28
30
32
34
36
0
.1
.2
.3
.4
.5
.6
.7
.8
.9
1.0
1.1
1.2

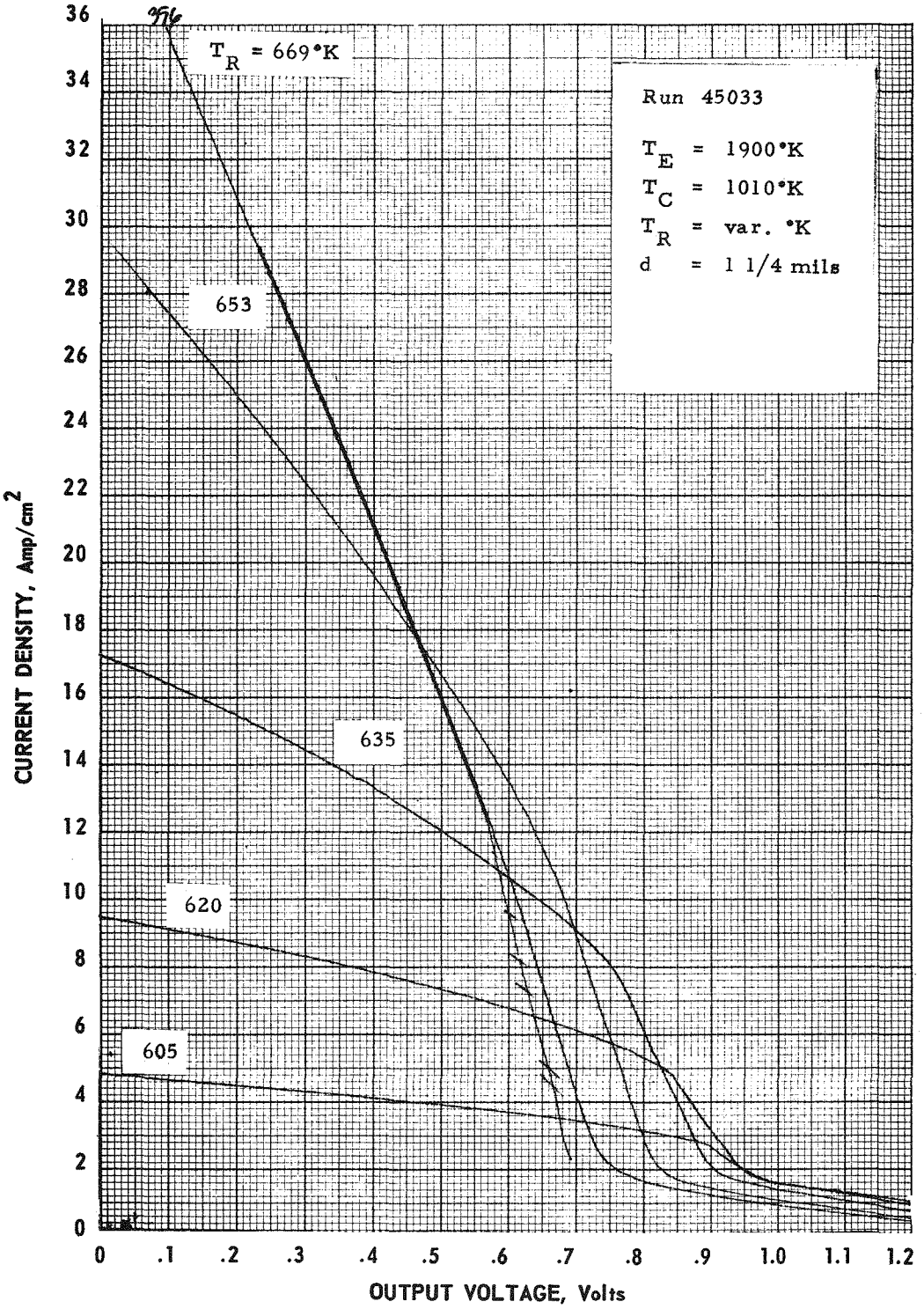
T_R = 669°K
Run 45033
T_E = 1900°K
T_C = 1010°K
T_R = var. °K
d = 1 1/4 mils
653
635
620
605
CURRENT DENSITY, Amp/cm^2
OUTPUT VOLTAGE, Volts
0
2
4
6
8
10
12
14
16
18
20
22
24
26
28
30
32
34
36
.1
.2
.3
.4
.5
.6
.7
.8
.9
1.0
1.1
1.2

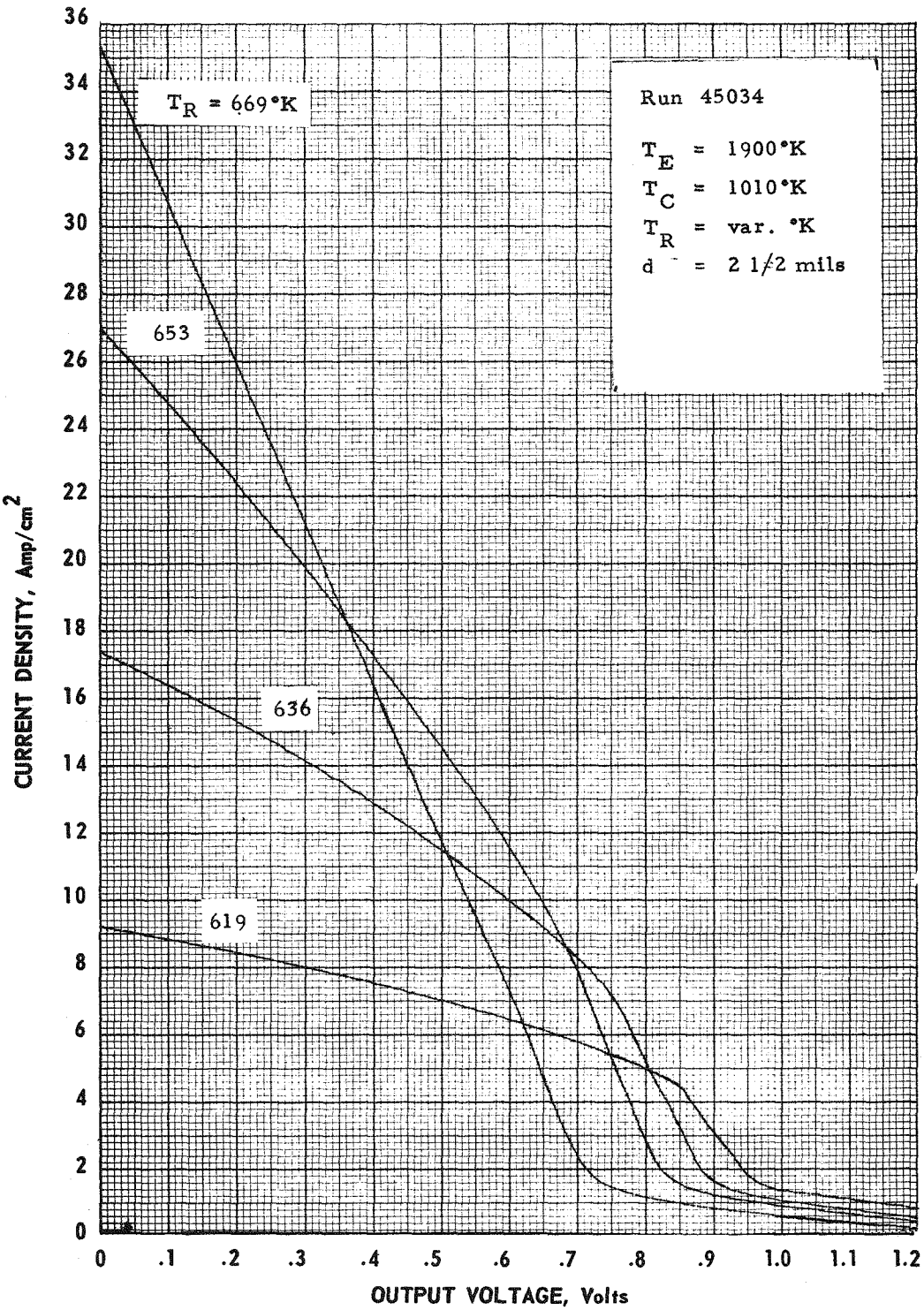
Run 45034
T_E = 1900°K
T_C = 1010°K
T_R = var. °K
d = 2 1/2 mils
T_R = 669°K
653
636
619
CURRENT DENSITY, Amp/cm^2
OUTPUT VOLTAGE, Volts
0
2
4
6
8
10
12
14
16
18
20
22
24
26
28
30
32
34
36
0
.1
.2
.3
.4
.5
.6
.7
.8
.9
1.0
1.1
1.2

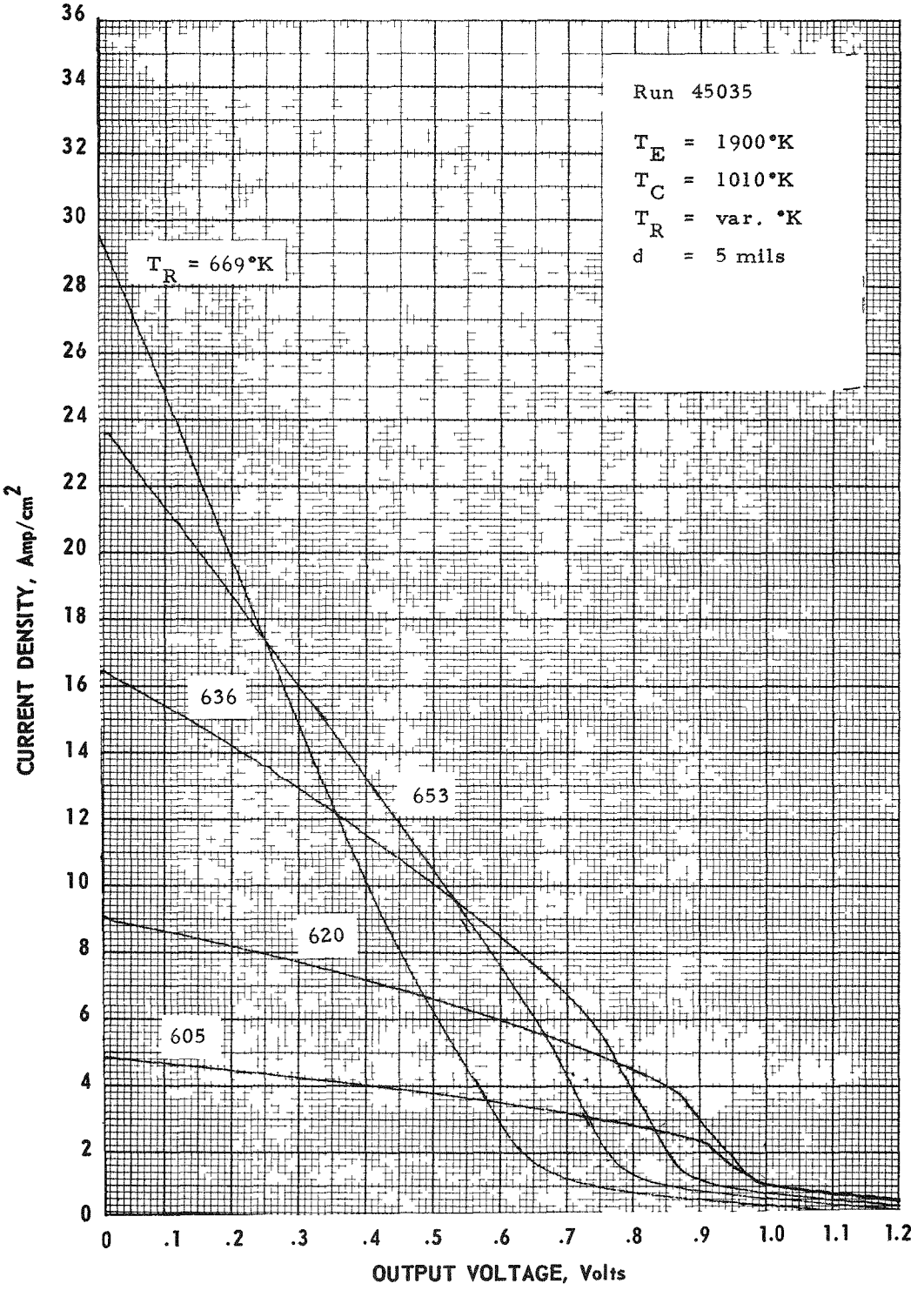
Run 45035
T_E = 1900°K
T_C = 1010°K
T_R = var. °K
d = 5 mils
T_R = 669°K
636
653
620
605
CURRENT DENSITY, Amp/cm^2
OUTPUT VOLTAGE, Volts
0
2
4
6
8
10
12
14
16
18
20
22
24
26
28
30
32
34
36
0
.1
.2
.3
.4
.5
.6
.7
.8
.9
1.0
1.1
1.2

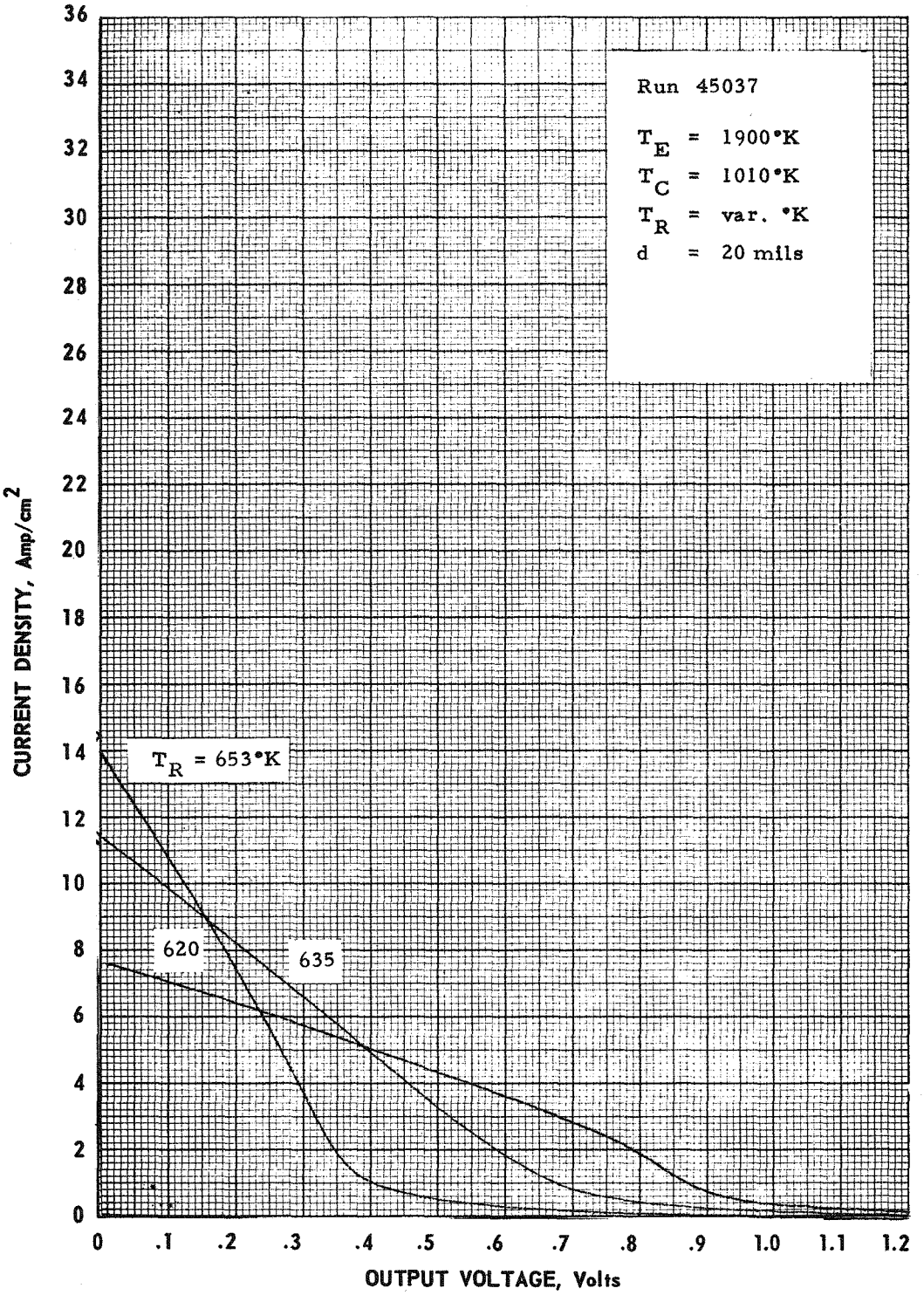
Run 45037
T_E = 1900°K
T_C = 1010°K
T_R = var. °K
d = 20 mils
T_R = 653°K
620
635
CURRENT DENSITY, Amp/cm^2
OUTPUT VOLTAGE, Volts
0
2
4
6
8
10
12
14
16
18
20
22
24
26
28
30
32
34
36
0
.1
.2
.3
.4
.5
.6
.7
.8
.9
1.0
1.1
1.2

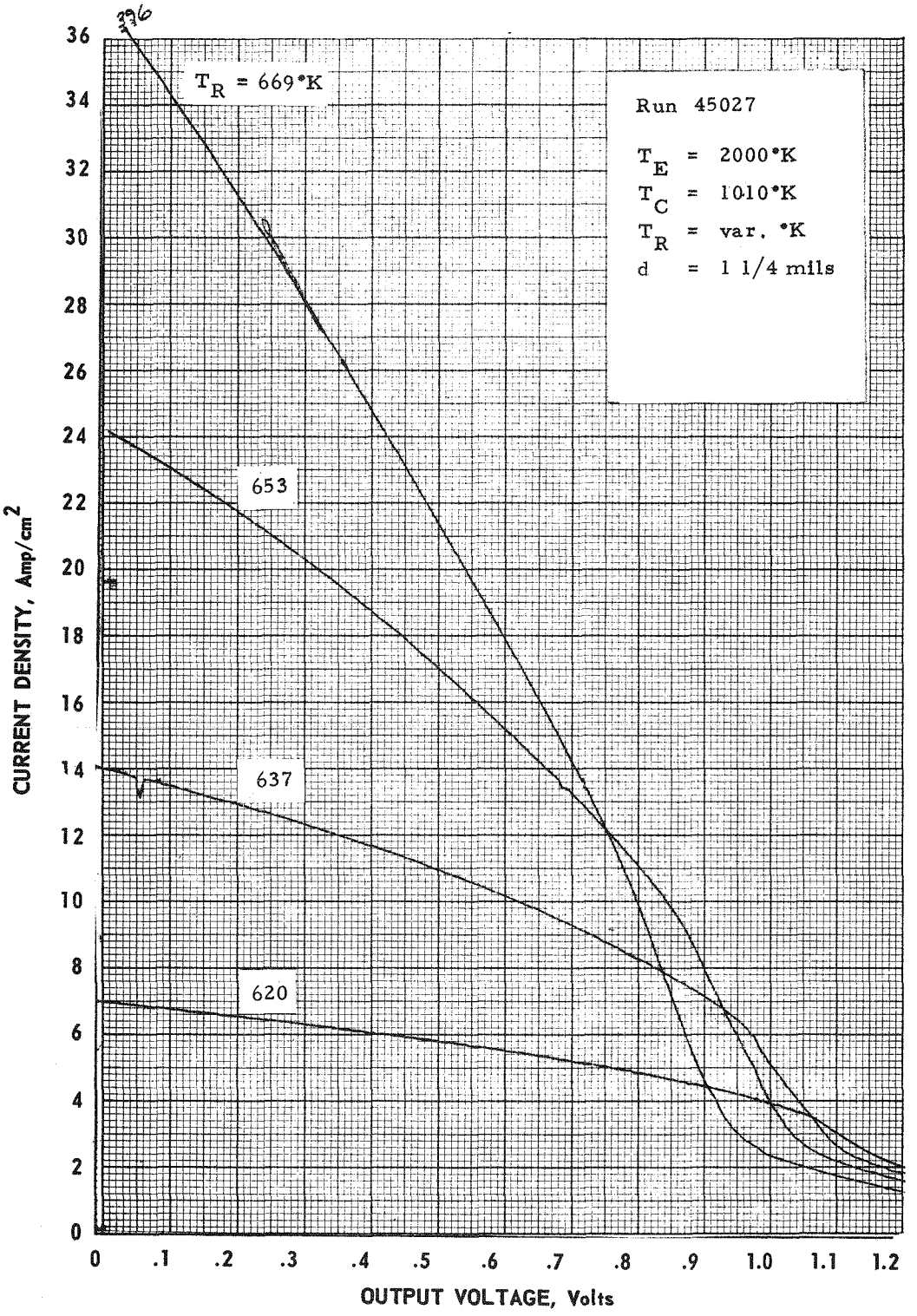
Run 45027
T_E = 2000°K
T_C = 1010°K
T_R = var. °K
d = 1 1/4 mils
T_R = 669°K
653
637
620
CURRENT DENSITY, Amp/cm^2
OUTPUT VOLTAGE, Volts
0
2
4
6
8
10
12
14
16
18
20
22
24
26
28
30
32
34
36
.1
.2
.3
.4
.5
.6
.7
.8
.9
1.0
1.1
1.2

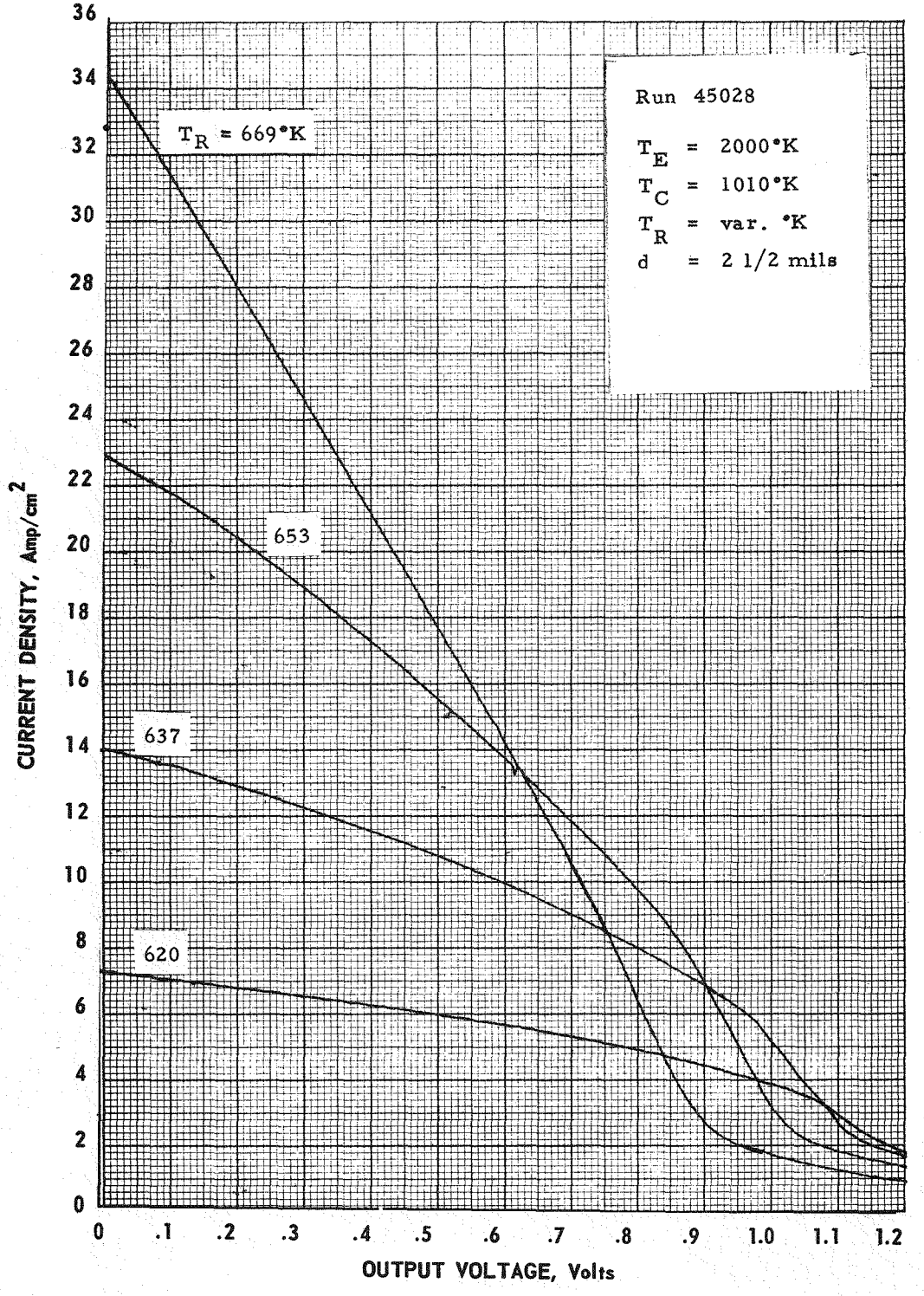
Run 45028
T_E = 2000°K
T_C = 1010°K
T_R = var. °K
d = 2 1/2 mils
T_R = 669°K
653
637
620
CURRENT DENSITY, Amp/cm^2
OUTPUT VOLTAGE, Volts
0
2
4
6
8
10
12
14
16
18
20
22
24
26
28
30
32
34
36
.1
.2
.3
.4
.5
.6
.7
.8
.9
1.0
1.1
1.2

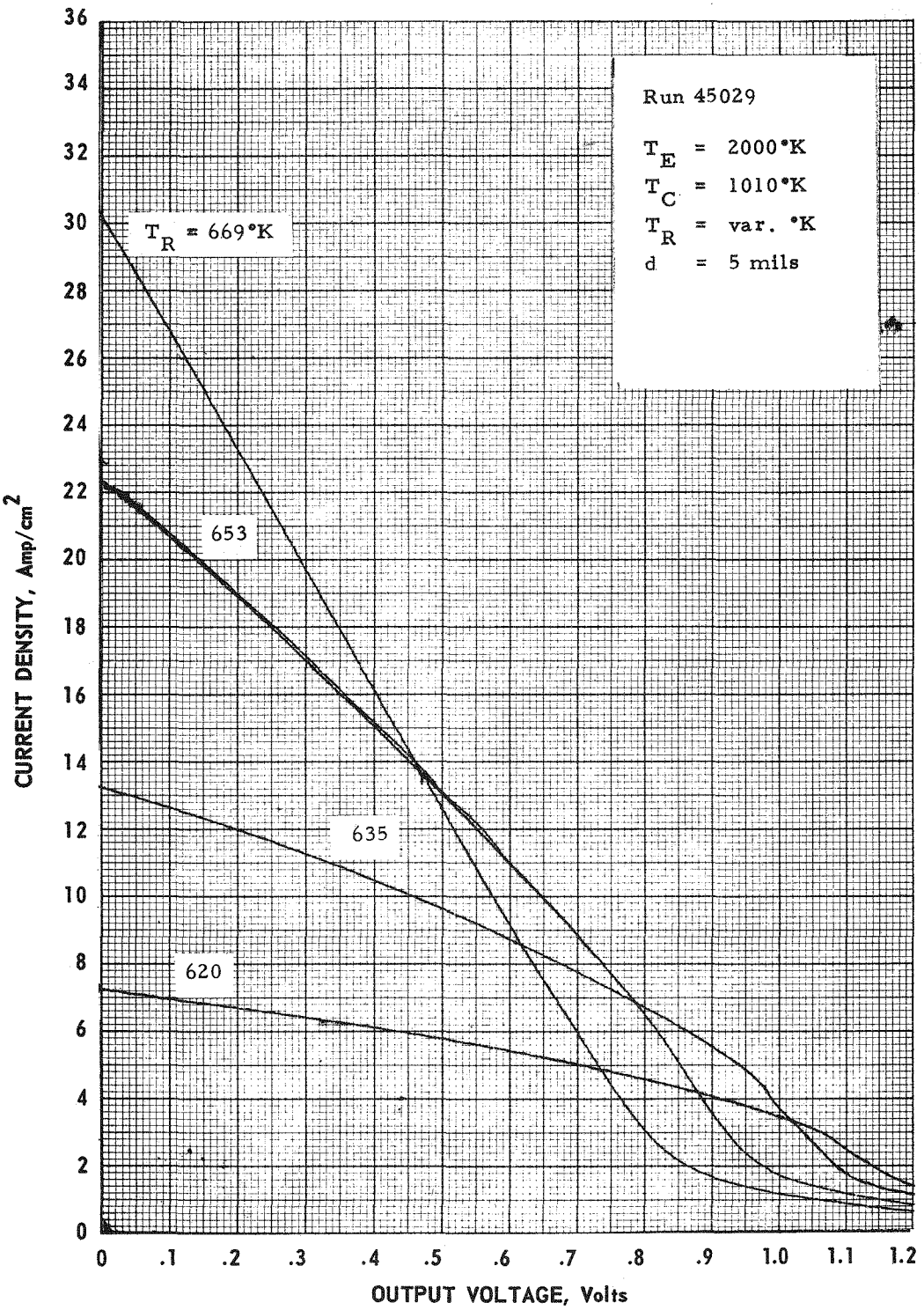
Run 45029
T_E = 2000°K
T_C = 1010°K
T_R = var. °K
d = 5 mils
T_R = 669°K
653
635
620
CURRENT DENSITY, Amp/cm^2
OUTPUT VOLTAGE, Volts
0
2
4
6
8
10
12
14
16
18
20
22
24
26
28
30
32
34
36
0
.1
.2
.3
.4
.5
.6
.7
.8
.9
1.0
1.1
1.2

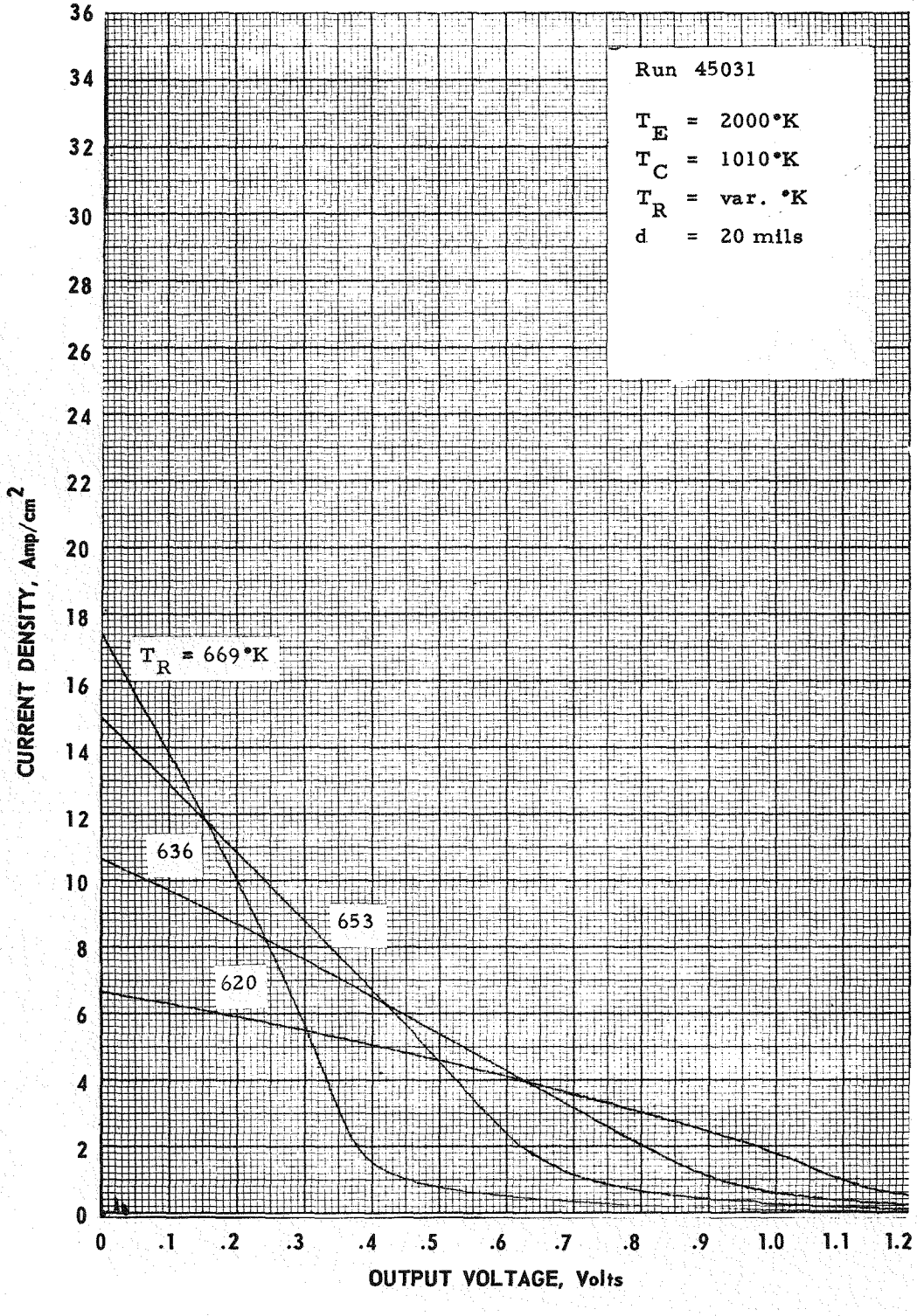
Run 45031
T_E = 2000°K
T_C = 1010°K
T_R = var. °K
d = 20 mils
T_R = 669°K
636
653
620
CURRENT DENSITY, Amp/cm^2
OUTPUT VOLTAGE, Volts
0
2
4
6
8
10
12
14
16
18
20
22
24
26
28
30
32
34
36
0
.1
.2
.3
.4
.5
.6
.7
.8
.9
1.0
1.1
1.2